

Reply to the Review of the Referee #1 (Bourbonnais)

(**RC**: Referee Comment; **AR**: Author's Responds)

First of all, thank you very much for thoroughly reviewing our manuscript and for the helpful comments and suggestions. We try to include as many comments and suggestions as possible which help us to improve our manuscript.

Abstract

Page 1, line 20

RC: $N^* < -1 \mu\text{M}$ is not a strong N deficit relatively to other regions of the ocean where N deficit is close to $40 \mu\text{M}$ (see Bourbonnais et al., 2015). What is the analytical error on their N^* estimate? Also, indicate depth of the minimum N^* .

AR: I agree with you that in comparison with other regions an N^* of $< -1 \mu\text{M}$ is not really a strong N deficit, but with lowest values of $-4 \mu\text{M}$ within the IDW (Page 14, lines 4-5) these values are significant in our study area. The analytical error on our N^* estimate based on the relative error of nitrate and phosphate analyses was below 1.5 % for duplicate sample measurements (Page 5, lines 12-13). The N^* Minimum is located within the RSPGIW and the IDW at a core depth of $\sim 1500 \text{ m}$ and ranged from $\sim 1000 \text{ m}$ until $\sim 1600 \text{ m}$ (Page 5, lines 12-13). This information will be added to the abstract.

Page 1, lines 23-24

RC: Indicate how the contribution from N_2 -fixation was estimated (i.e., using N/P and Redfield ratio assumptions).

AR: We are using a simple calculation for a first estimate of the input of new nitrate into the surface layer by N_2 -fixation by using the deviation of the N/P-Redfield-ratio. We will clarify this in the revised version.

Introduction

Page 2, line 12

RC: The transition is awkward. Rewrite.

AR: We modified the sentence to: "To study the marine nitrogen cycle, we use nitrate and phosphate concentrations as well as the isotopic signature of nitrate (Deutsch et al., 2001; Deutsch et al., 2007; Gruber and Sarmiento, 1997; Lehmann et al., 2005; Sigman et al., 2005)."

Page 2, lines 20-22

RC: One important caveat is that N^* cannot be used to derive rates of N_2 -fixation in region where denitrification co-occurs, as the N^* signatures associated with denitrification and N_2 -fixation are overprinting each other's. One advantage of measuring the dual isotopic composition of nitrate is that it allows disentangling these different overprinting processes, because, as stated later in the

manuscript, N₂-fixation is associated with negative N to O nitrate isotope anomalies. On the other hand, denitrification is not expected to produce such N to O nitrate isotope anomalies because N and O are equally fractionated during this process. This point should be better emphasized in the introduction (and better exploited in their discussion).

AR: You are right that in regions where denitrification and N₂-fixation simultaneously occur N* cannot be used alone. However, in our study area no denitrification takes place and we just see a signal in intermediate and deep waters coming from the Arabian Sea, where denitrification take place. We use the positive surface N* signatures as a first evidence for N₂-fixation and confirm these signatures with the distinct upward decrease of N-isotope values compared to strongly elevated $\delta^{15}\text{N}$ values in subsurface waters (~500 m, elevation of ~2-3.5 ‰). I agree that dual isotope measurements of nitrate will help to improve the weakness associated with the N* approach and we will rewrite and add a section on dual isotopes.

Page 2, lines 28-29

RC: Change for: "lighter isotopes are preferentially assimilated, leaving the substrate enriched in ¹⁵N and ¹⁸O."

AR: This sentence will be rewritten as you noted.

Page 3, line 1

RC: Add references here, e.g., Knapp et al., 2008 and Bourbonnais et al., 2009.

AR: We will add these references.

Page 3, line 4

RC: Which depth range corresponds to $\delta^{15}\text{N}_{\text{deep}}$ and $\delta^{18}\text{O}_{\text{deep}}$?

AR: For $\delta^{15}\text{N}_{\text{deep}}$ and $\delta^{18}\text{O}_{\text{deep}}$ we use the mean of $\delta^{15}\text{N}$ and $\delta^{18}\text{O}$ within the water depth below 2000 m. When we will still use the tracer $\Delta(15,18)$ (see explanation below) we will add this information in the introduction part and in the discussion section on Page 18, line 1.

Page 3, lines 14-16

RC: Be more specific about the new findings from this study. Which specific gaps were filled comparatively to previous studies?

AR: We will explain more precisely that our findings filled the gaps between the mentioned studies relating to nutrient distribution, nitrate isotope measurements and water mass analyses. First, in this region, we linked the different water masses of different origin with their isotopic signature. We will clarify our new findings in the revised version.

Materials and Methods

Page 6, line 13

RC: Why using a single point correction only?

AC: We will correct the method section, because we indeed do not use a single point correction but rather a two-point correction referred to IAEA-N3 ($\delta^{15}\text{N-NO}_3^- = +4.7\text{‰}$ and $\delta^{18}\text{O-NO}_3^- = +25.6\text{‰}$) and USGS-34 ($\delta^{15}\text{N-NO}_3^- = -1.8\text{‰}$ and $\delta^{18}\text{O-NO}_3^- = -27.9\text{‰}$) for $\delta^{15}\text{N-NO}_3^-$ and $\delta^{18}\text{O-NO}_3^-$.

Page 6, line 15

RC: What was blank size?

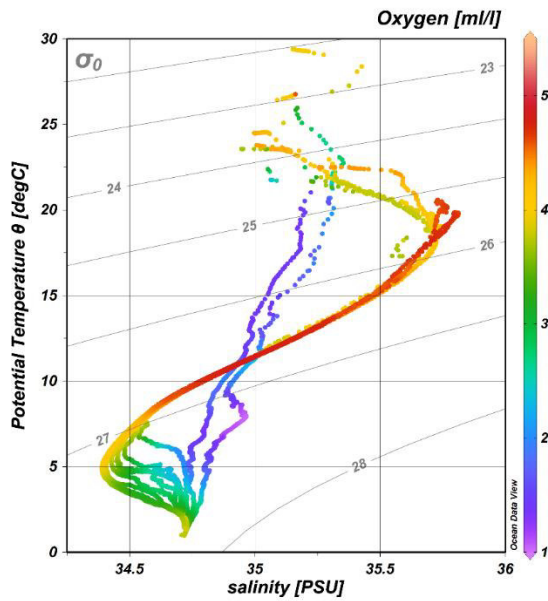
AR: The standard deviation for IAEA-N3 was generally better than 0.2 ‰ for $\delta^{15}\text{N-NO}_3^-$ and 0.3 ‰ for $\delta^{18}\text{O-NO}_3^-$, which is within the same specification for $\delta^{15}\text{N-NO}_3^-$ and $\delta^{18}\text{O-NO}_3^-$ for at least duplicate measurements of the samples.

Results

Page 6, section 3.1

RC: It would be helpful to show T-S diagrams at this point rather than later in the discussion.

AR: We thought about the best position of the Sigma-theta-Salinity and Sigma-theta-Oxygen diagrams within our manuscript. In the end, we decided to show these diagrams with the distinct classification of the different water masses and the resultant water mass distribution model in a separate discussion section because of the high portion of discussion rather than just the presentation of results. In our water mass analyses, we use many different sources, describing water masses in the world's ocean and when available from expeditions in the Indian Ocean, but they are quite rare and no water mass model existed for our study area. Therefore, we decided to present the water mass distributions in an own discussion section and not as a part of the results. Consequently, the diagrams with the clear water mass classification along their density surfaces belong more to the discussion section. However, it would be a good opportunity to show a typical T-S diagram (see example below in addition to the salinity and oxygen color sections in Figures 2 a and b) in the results. These will give a first overview about the differences between northern and southern water masses and introduce the Figures and detailed explanation in the discussion part. This might be a good consensus.

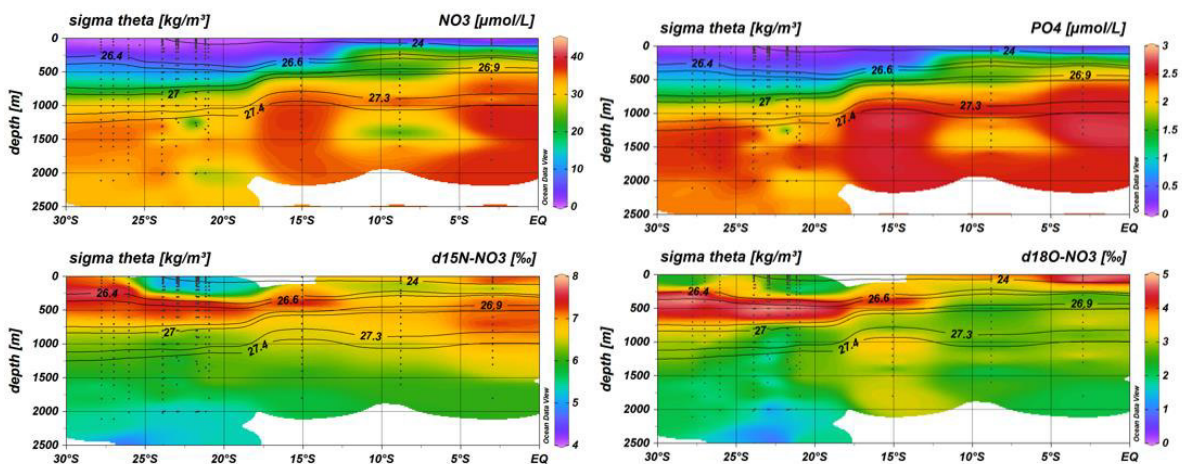


Example for a T-S-diagram

Page 7, lines 6-16 and Page 8, lines 2-13

RC: Figure 5 (panels a, b, c, d) should be presented in this section and Table 2 moved to the supplementary materials. Figure 5 (panels e, and f) should be presented in this section and Table 3 moved to the supplementary materials.

AR: If we move Figure 5 to the results we will have to remove the overlay of water mass boundaries in the panels because they were added as a consequence of the water mass discussion section. Above we explained why we decided to present our water mass analyses as a part of the discussion. An opportunity to leave Figure 5 (a-f) in section 4.2.1 and to accommodate with your remarks is to add only nitrate and phosphate, and N and O isotope sections (see example below; like Figure 2a and b for salinity and oxygen) to the results (3.2) and move Table 2 and 3 to the supplementary materials.



Example for nitrate, phosphate and N and O isotope transects

Discussion

Page 9, line 6-7

RC: What is new in their water mass distribution model (Figure 4)?

AR: This is the first water mass distribution model for this region, for further explanation see response above for “page 6, section 3.1”

Page 9, lines 25-26

RC: Change for “... because of respiration and the absence of effective ventilation...”

AR: We will rewrite the sentence as you mentioned.

Page 9-12:

RC: It would be useful to include the nitrate isotopic composition (end-members) for the different water masses, either in Figure 4, or in a Table.

AR: This is a good annotation. A type of endmembers are shown in Table 3 where the mean $\delta^{15}\text{N}$ and $\delta^{18}\text{O}$ are presented for different latitudes (because the water mass distribution changes along the transect) and for different water depth representing the different water masses. We can modify this Table and add the water masses for a better overview. Then we can move this Table to the beginning of section 4.2.1, after the water mass discussion part. It would be better to represent this new “end-member Table” for nitrate isotopes in section 4.2.1 rather than in section 3.1, because for the first time we connect the water masses and the results of the nutrient and isotopic measurements in section 4.2.1. This Table would then nicely correspond to Figure 5(a-f).

Page 12, lines 20-21

RC: The $\text{NO}_3^-/\text{PO}_4^{3-}$ should however increase if N_2 -fixation is significant.

AR: Enhanced N/P ratios in N-fixing organisms has been reported and would introduce these enhanced N/P ratios also to the water mass as the N-fixers are mineralised. This process is reflected in enhanced N/P ratios. The way we calculated the contribution from N_2 -fixation is thus a minimum estimate of N contribution from N_2 -fixation. If part of the P was also from N-fixers and if the N/P ratio of N fixers was known, their contribution could have been better estimated. However, we are not sure about the N-fixers N/P ratio. We will, however, examine this carefully in the revised version and improve this part including the dual isotope approach.

Page 13, lines 10-11

RC: How does the mean $\text{NO}_3^-/\text{PO}_4^{3-}$ ratio changes along the latitudinal transect? What are the implications for N_2 fixation?

AR: The change of N/P ratio along the latitudinal transect is presented in Figure 5c and demonstrates the oligotrophic regime in the subtropical gyre. Implications for N_2 -Fixation are: (1) Elevated N^* values of $>2 \mu\text{M}$ in surface

waters south of $\sim 15^{\circ}\text{S}$. (2) We observe distinctly lower $\delta^{15}\text{N}$ values ($<4.5\text{-}5.0\text{‰}$) in the surface waters compared to the subsurface values within the SAMW with values of $>7\text{‰}$ and highest values of $\sim 8\text{‰}$. This leads to a $\delta^{15}\text{N}$ difference of $2\text{-}3.5\text{‰}$, which is similar to the difference in other studies, i.e. Bourbonnais et al. (2009) with a difference of 3‰ (from 5‰ to 2‰). Our surface $\delta^{15}\text{N}$ values are also slightly lower than the average $\delta^{15}\text{N}$ values of depth water nitrate ($>2000\text{ m}$; 5.5‰). (3) We estimated in your simple calculation the input of new nitrate into the surface layer by N_2 -fixation and demonstrated the increase of the N/P ratio of completely assimilated nitrate (Figure 9a).

Page 14, line 1 and Page 18, line 16

RC: Bourbonnais et al. (2009) is incorrectly referenced here.

AR: We apologize for the incorrectly referenced study. We will correct this.

Page 15, lines 5-6

RC: Add references to support this statement.

AR: We will add references.

Page 16, lines 17-18

RC: Why nitrate utilization is unlikely? It is too deep?

AR: It is to our knowledge a clear mixing signal that causes the moderate slopes of $\delta^{15}\text{N}/\ln(\text{NO}_3)$ in both the gyre region and in the Subantarctic and we think that nitrate utilization is unlikely at this depth. Sigman et al. (2000) also described the mixing of different end-members along the SAMW from the Antarctic with higher $\delta^{15}\text{N}$ (up to 13‰) values and lower $\delta^{15}\text{N}$ ($<6\text{‰}$, Liu et al., 1996) values towards lower latitudes.

Page 18, lines 21-24

RC: Bourbonnais et al. (2009) report a range of 2 to 5‰ for the $\delta^{15}\text{N}$ of nitrate in surface waters of the subtropical northeast Atlantic Ocean. Using a simple isotopic mass balance, they estimated that N_2 fixation could account for up to 40% of the export production in this region.

AR: This agrees with our $\delta^{15}\text{N}$ values, which are between 4.5 and 5.0‰ in surface waters and we estimated that N_2 -fixation could account for $\sim 30\%$ of the export production. We will clarify this in the revised version.

Page 18, lines 29-31

RC: It is peculiar to note that the $\Delta(15,18)$ anomalies observed in this studies are at least half of the anomalies observed in the subtropical northeast Atlantic Ocean by Bourbonnais et al. (2009) ($\Delta(15,18)$ of -7 to 0‰). Why would that be if the estimated contribution from N_2 fixation is supposedly in the same range (accounting for $30\text{-}40\%$ of new supplied nitrate) for these two regions? The N^* observed by Bourbonnais et al. (2009) was also up to $\sim 3.5\text{ }\mu\text{mol}/\text{kg}$.

AR: We will carefully examine this in the revised version using the suggested literature and include a discussion on the dual isotopes. We will reconsider the use of tracer $\Delta(15,18)$ because of the diverse source waters. Better would be the tracer $\Delta(15-18)$ from Rafter et al. (2013), who used only the difference between N and O isotope signatures which is more useful in regions characterised by a variety of water masses. We will consider this in the revised version.

Page 19, lines 8-9

RC: In equation (6), the nitrate to phosphate ratio ($\text{NO}_3^-/\text{PO}_4^{3-}$) is divided by the measured phosphate concentrations, not multiplied.

AR: You are right, the equation is incorrect and N/P_{cal} must be multiplied by the phosphate concentrations. Sorry for this mistake.

Page 19, lines 1-23

RC: This approach requires many assumptions. One likely invalid assumption is assuming a Redfield ratio of 16. The Redfield ratio is variable in marine microalgae (see Geider et al., 2002). N_2 fixers also have higher N/P ratios (e.g., Letelier et al., 1998). Finally, this approach does not take into account inputs from atmospheric depositions.

AR: Because N_2 -fixers have higher N/P ratios, we calculated the assimilated nitrate by representing the deviation from the Redfield stoichiometry of 16:1 and therefore the higher N/P ratios of the assimilated nitrate are an evidence for N_2 -fixation in surface waters (see comment above). We believe that we have presented a minimum estimate by our calculation but will re-examine our approach and try to find a better way to estimate the N-contribution by nitrogen fixers. We will check the literature on atmospheric deposition but we think that it is quite small in the study area as sinking particles and sediment have only little lithogenic material.

Page 19, line 21

RC: This is confusing, as $\delta^{15}\text{N-NO}_3\text{-fix}$ (i.e. supplied from N_2 fixation) should be about 0‰. I suggest removing the “fix” subscript.

AR: We agree with this remark, that $\delta^{15}\text{N-NO}_3\text{-fix}$ is confusing; we will remove the subscript “fix”.

Page 19, lines 20-23

RC: Overall, the dual nitrate isotopic data could be better exploited in their discussion and used in an isotopic box model to derive an independent assessment of the contribution from N_2 fixation (see examples from Knapp et al., 2008 and Bourbonnais et al., 2009).

AR: Our simple estimation on N_2 -fixation is the first try to get an impression on the input of new nitrate into the system of the subtropical gyre in the South Indian Ocean. For a box model we need to combine or water column analyses with the result of suspended matter samples and particle flux samples from sediment

traps. For this study, we first wanted to demonstrate the diversity of water masses in the less explored subtropical gyre of the South Indian Ocean and second, to highlight their varying influence on the nutrient and isotopic composition, which is likewise less investigated in this region. Our simple estimation on N₂-fixation is a first approach on the input of new nitrate into this special oligotrophic region. We will include the dual isotopes to strengthen our point on N-fixer contribution.

Page 20, lines 9-10

RC: Bourbonnais et al. (2009) did not observe significant positive $\Delta(15,18)$ anomalies in the subtropical northeast Atlantic Ocean. Which make me wonder what is the propagated (analytical) error associated with their $\Delta(15,18)$ measurements. In other words, is their calculated positive $\Delta(15,18)$ significantly different from 0?

AR: See above: We will consider to use the tracer $\Delta(15-18)$ instead of $\Delta(15,18)$ and agree that a $\Delta(15,18)$ of +0.5 or -0.5 ‰ is not a significant amplitude.

Page 20, line 16

RC: N₂-fixation have been shown to occur at lower temperatures in temperate regions (see Moisander et al., 2010).

AR: The sudden change in $\delta^{15}\text{N}$ and N* is difficult to explain in the gyre as nutrients are not increasing. We have no data on micronutrients but find it unlikely that these change significantly within the gyre. Therefore, the only feasible explanation seems to be the temperature drop. However, we will stress the contradictory literature in the revised version.

Tables

Table 1

RC: It is not necessary since the information is already presented in Figure 1. I recommend moving it to the supplementary materials.

AR: Table 1 will be moved to the supplement.

Table 2 and 3

RC: Should be moved to the supplementary materials as this information is already in Figures 3 and 5.

AR: See comment to Page 7, lines 6-16 and Page 8, lines 2-13

Figures

Figure 1

RC: It is difficult to see the shaded arrow representing the South equatorial current.

AR: We will highlight the shaded arrow by adding a contour line.

Figure 6

RC: What is the r^2 and error on the slope?

AR: r^2 is 0,99. We will add the r^2 and the error of the slope in the revised version.

Figure 7b

RC: Which processes cause the positive $\Delta(15,18)$?

AR: See Sigman et al (2005): Nitrification/Remineralisation cycle in deeper waters leads to a slightly positive in $\Delta(15,18)$. We will add more information on that in the revised version.

Technical comments

Page 1, lines 30-31 and Page 2, line 2

RC: This sentence is repetitive. Replace by something like: "The South Indian Ocean is dominated by a subtropical anticyclonic gyre (refs), the Indian Ocean subtropical gyre" (IOSG), one of the major subtropical gyres in the world's ocean. The IOSG has been, thus far, sparsely investigated." Use the IOSG acronym defined earlier.

AR: We will rewrite the sentence as you mentioned and define the "IOSG" acronym earlier in the text.

Page 3, line 10

RC: Remove "Therefore" at the beginning of sentence.

AR: We will remove the "therefore".

Page 12, line 7

RC: Change for "nutrient distribution and N cycle processes"

AR: We will change the headline as you mentioned.

Reply to the Review of the Referee #2 (Anonymous)

(**RC**: Referee Comment; **AR**: Author's Responds)

First of all, thank you very much for reviewing our manuscript thoroughly and for the helpful comments and suggestions. We try to include as many comments and suggestions as possible which help us to improve our manuscript.

Abstract

Page 1, line 20

RC: I would remove 'strong' here, as N^* of $-1 \mu M$ would not generally be considered "a strong N deficit".

AR: We agree with you and have omitted "strong" here.

Page 1, lines 21-23

RC: Please clarify what you are referring to here using "preformed versus regenerated". The preceding sentence referred to nitrate isotope signals coming from SAMW and from denitrification in the Arabian Sea. Where is the 'regenerated' signal that you are referring to?

AR: The nitrate that is added by N_2 -fixation and immediately consumed (assimilated) in the surface layer is meant as regenerated nitrate, as well as the remineralised nitrate by nitrification. These are in situ processes contrary to the preformed isotopic composition of nitrate induced by the lateral influence from the neighbouring water masses. We will rewrite the sentence to make this clearer.

Page 1, lines 23-25

RC: If there is significant N_2 fixation, I would not expect low nitrate to phosphate ratios. Revisit the N_2 fixation discussion below.

AR: Enhanced N/P ratios in N-fixing organisms has been reported and would introduce these enhanced N/P ratios also to the water mass as the N-fixers are mineralised. This process is reflected in enhanced N/P ratios. The way we calculated the contribution from N_2 -fixation is thus a minimum estimate of N contribution from N_2 -fixation. If part of the P was also from N-fixers and if the N/P ratio of N fixers was known, their contribution could have been better estimated. However, we cannot be sure about the N-fixers N/P ratio. We will, however, examine this carefully in the revised version and improve this part including the dual isotope approach.

Introduction

Page 2, line 21

RC: I think a reference to Gruber and Sarmiento, 1997 would be appropriate here.

AR: We will add the reference of Gruber and Sarmiento (1997).

Page 2, lines 29-30

RC: The isotopic fractionation factor, ϵ , relates the instantaneous product, not the accumulated product, to the substrate. Though neither is explicitly stated, I think the implication is that this always holds true. This should be clarified.

AR: We will examine this carefully and clarify this in our revised version.

Materials and Methods

Page 6, line 14

RC: How is the 'single point correction' for $\delta^{15}\text{N}$ applied? Is this simply a standard subtraction?

AR: We will correct the method section, because we indeed do not use a single point correction but rather a two-point correction referred to IAEA-N3 ($\delta^{15}\text{N-NO}_3^- = +4.7\text{‰}$ and $\delta^{18}\text{O-NO}_3^- = +25.6\text{‰}$) and USGS-34 ($\delta^{15}\text{N-NO}_3^- = -1.8\text{‰}$ and $\delta^{18}\text{O-NO}_3^- = -27.9\text{‰}$) for $\delta^{15}\text{N-NO}_3^-$ and $\delta^{18}\text{O-NO}_3^-$.

Results

Page 6, line 29

RC: What water mass does the 34.6 PSU feature represent?

AR: AAIW (Antarctic Intermediate Water) is characterised by a salinity minimum of <34.6 PSU at a core density of 27.2 kg/m³. There is a mistake on page 10, line 2: "The salinity minimum (<34.9 PSU) south of 15° S ...". We will correct this to "The salinity minimum (<34.6 PSU) south of 15° S...". Sorry for this misunderstanding.

Figure 2

RC: It might be more helpful to include contours for the potential density surfaces, rather than contouring the same properties represented on the color bar.

AR: This is a good remark and is a chance to include more information into the sections. We will change the contour lines for the potential density surfaces.

Pages 7 and 8

RC:

(1) I don't understand the choices behind what is shown in Tables 2 and 3. Why are these specific density/depth intervals selected, and why look at different density levels in the different latitude zones? Why are only one nitrate and

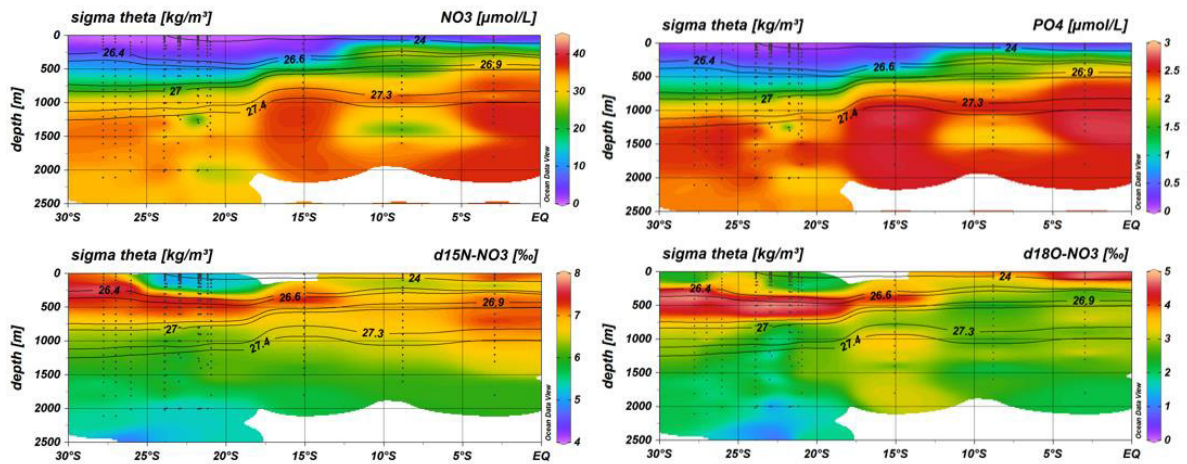
phosphate concentration (Table 2) or nitrate $\delta^{15}\text{N}$ and $\delta^{18}\text{O}$ value (Table 3) given for each line? How many measurements are included in these values? Shouldn't there be a range or uncertainty given for these if they derive from a range in latitude?

(2) Throughout this presentation of results in sections 3.2 and 3.3, I found referring to Figure 5 more useful than consulting Tables 2 and 3. I would suggest moving Figure 5 earlier in the paper, and removing Tables 2 and 3, or perhaps moving them to the supplement, unless their relevance can be better explained.

AR:

(1) For Table 2 and 3 we chose these depth intervals to provide average nitrate/phosphate concentrations (Table 2) and $\delta^{15}\text{N}/\delta^{18}\text{O}$ values (Table 3) for each water mass (along sigma-theta surfaces) in their specific latitudinal extent and thickness. Because the water mass distribution changes along the latitudinal transect, we chose 3 or 4 different latitudinal clusters to represent the change of nitrate/phosphate concentrations in Table 2 and isotopic compositions in Table 3. In Table 3 we decided to add a fourth latitudinal cluster to represent the divergent higher $\delta^{15}\text{N}$ and $\delta^{18}\text{O}$ values between 27.78°S and 26.05°S . For a better understanding of these Tables, it might be better to show the sigma-theta intervals rather than the depth intervals and to add the associated water masses to the density surfaces in the specific latitudinal section. We showed only one value for each latitude and depth range because these are averages of one to ten single values. You are right that we have to add a range for the average values. The uncertainties of each single measurement are shown in the supplement Table S1 and S2.

(2) If we move Figure 5 into the results we have to remove the overlay of water mass boundaries in the panels, because they were added as a consequence of the water mass discussion section. We thought intensely discussed this issue with all co-authors where the best position of the water mass section would be within our manuscript. In the end, we decided to present this section with the distinct classification of the different water masses and the resultant water mass distribution model in a separate discussion section because of the high portion of discussion rather than just the presentation of results. In our water mass analyses, we use many different sources, describing water masses in the world's ocean and when available from expedition in the Indian Ocean, but they are quite rare and no water mass model existed for our study area. Therefore, we decided to present the water mass distributions in an own discussion section and not as a part of the results. Consequently, we think that, Figure 5 with the overlying water mass distribution belongs to the discussion section. However, it would be a good opportunity to leave Figure 5 (a-f) in section 4.2.1, but add only nitrate, phosphate and nitrate isotope color sections without overlying water mass distributions (see example below; like Figure 2a and b for salinity and oxygen) to the results (3.2) and move the reworked Tables 2 and 3 to the supplementary materials.



Example for nitrate, phosphate and N and O isotope transects

Page 7, line 6

RC: I would delete ‘strongly’. When working in oligotrophic areas, I’m not sure 5.9 μM nitrate qualifies as “strongly depleted”. Otherwise, you could perhaps cite the concentration of nitrate in the surface waters, rather than at 310 m.

AR: This is a good objection. We will rewrite the sentence.

Discussion

Page 10, line 27

RC: Please clarify “decrease of the oxygen minimum”. Do you mean that the oxygen concentration is increasing? If so, please rephrase.

AR: Yes, “decrease of the oxygen minimum”, means that the oxygen concentration increases, we will rephrase the sentence.

Figure 3

RC: I didn’t find this Figure necessary, and suggest that it be moved to the supplement.

AR: This Figure is intended to show how we defined the different water mass boundaries and how the water mass distribution model was generated. We think the presentation of these diagrams is very important for our water mass analyses and we would like to leave this Figure in the main text, unless you would necessarily move the Figure to the supplement.

Figure 4

RC: I think this Figure is extremely helpful for thinking about the water mass structure of the region! My only question is what determines where the lines dividing water masses are drawn? Are these specific sigma theta surfaces? Please clarify.

AR: To generate this water mass distribution model we use sigma-theta surfaces, and salinity and oxygen distribution (see Figure 3) to define the different water masses in the latitudinal transect. We separate the transect in

three latitudinal sections (see Figure 3): 20.36-27.78°S, 15.08°S and 2.98-8.81°S to represent the change of the water mass distribution along our transect. Therefore, we thought the presentation of Figure 3 helps to understand the generation of Figure 4.

Figure 6

RC: The Figure legend states that the color bar indicates potential density, but what is actually used is depth. Perhaps sigma theta would, in fact, be better.

AR: Sorry for this mistake! First, the color bar represents sigma-theta and was changed later into a depth color bar without a correction of the Figure legend. We will correct this and change the color bar for sigma-theta.

Page 15, line 16

RC: Doesn't iron availability also play a role in incomplete nitrate assimilation in the Southern Ocean?

AR: We will consider this and rewrite this paragraph.

Page 17, line 3

RC: Please clarify "lower water depths". Do you mean shallower or deeper?

AR: Sorry for the misunderstanding, we meant shallower water depths. We will make this clearer.

Figure 8

RC: The yellow star representing the mean nitrate $\delta^{15}\text{N}$ does not stand out. I would suggest making this symbol a different color or shape. Also, please provide the slope of the solid line in the Figure legend.

AR: We will highlight more clearly the symbol for the mean nitrate $\delta^{15}\text{N}$ and add the slope of the solid line in the Figure legend.

Page 17, line 11

RC: Typo, should be 'SAMW' rather than "SAWM".

AR: We will correct this mistake.

Page 17, line 14

RC: Please give Sigman et al., 2005 reference to $\Delta(15,18)$. Rafter et al (2013) is also a good reference, but uses $\Delta(15-18)$ instead.

AR: In our revised version we will reconsider the use of $\Delta(15,18)$ because of the diverse source waters in our study area. Better would be the tracer $\Delta(15-18)$ from Rafter et al. (2013), who used only the difference between N and O isotope signatures which is more useful in regions characterised by a variety of water masses. We will consider this in the revised version.

Page 18, line 16

RC: I would include a reference here to Gruber and Sarmiento 1997 for their seminal work in this area.

AR: We will include the reference to Gruber and Sarmiento (1997) here.

Page 18, line 24

RC: One could also reference work in the Atlantic from Knapp et al., 2008, and a variety of work from the Pacific.

AR: We will consider this and add more information from studies in the Atlantic and Pacific (Knapp et al., 2008 and Bourbonnais et al. 2009, etc.)

Page 19, lines 7-8

RC: What are the implications of assuming Redfield stoichiometry here?

AC: We will examine and clarify this in the revised version.

Page 19, line 10

RC: This equation appears incomplete, if not incorrect. From the text, I would not expect PO₄³⁻-sample to appear in the denominator.

AR: Sorry for this mistake, you are right, the equation will be $NO_3^-_{cal} = NO_3^- / PO_4^{3-}_{cal} * PO_4^{3-}_{sample}$

Page 19, line 12

RC: What is the N:P ratio assumed for newly fixed N? This seems important to the calculations performed here.

AR: We assumed an elevated N/P ratio for newly fixed N compared to the preformed N/P ratio in our study area (13.25 in the IOSG and 14.25 in the south equatorial Indian Ocean). We observe these higher N/P ratios in our surface samples (low nitrate concentration of <5 μM) in Figure 9a.

Page 19, lines 20-23

RC: A newly fixed δ¹⁵N of 4.8‰ is not within the range of expected values for N₂ fixation. This seems problematic, and requires reevaluation and justification of the approach used to arrive at this value. In my mind, a value of +4.8‰ argues against this N deriving from N₂ fixation. What other explanations have the authors considered?

AR: Indeed, we found evidences for N₂-fixation: 1) Elevated N* values of >2 μM in surface waters south of ~15°S. (2) Even though a δ¹⁵N of 4.5 to 5.0 ‰ is not a clear evidence for the input of low δ¹⁵N by N₂-fixation, the distinct decrease from subsurface values within the SAMW with values of >7 ‰ and highest values of ~8 ‰ indicate an upward decrease of 2-3.5 ‰. This decrease can only be explained by the input of fixed N into the surface layer. Additionally, studies in the Atlantic indicate the similar difference of 3 ‰ (from 5 ‰ to 2 ‰), i.e Bourbonnais et al. (2009). Furthermore the surface δ¹⁵N values are lower than

the $\delta^{15}\text{N}$ deep water mean of >5.5 ‰. (3) The calculated value of $+4.8$ ‰ is just a simple calculation there we take the calculated 30% of new N-input by N_2 -fixation and compare this value with our observations assuming the SAMW as N source with a $\delta^{15}\text{N}$ of >7 ‰. When the source would have higher $\delta^{15}\text{N}$ values, than we would get higher $\delta^{15}\text{N}$ values for the newly fixed $\delta^{15}\text{N}$ in surface waters. In the revised version, we will make our arguments for N_2 -fixation clearer.

Figure 9

RC: It is difficult to distinguish the symbols used to represent the two geographic areas in panel a. What calculation is used to derive the grey line in panel a?

AR: We will choose different symbols for a better differentiation in Figure 9a. The grey solid line indicates the calculated N-assimilation (regression line of NO_3^- -cal vs. $\text{NO}_3^-/\text{PO}_4^{3-}$ -cal) with a preformed $\text{NO}_3^-/\text{PO}_4^{3-}$ -in ratio of 13.25 for the region of the IOSG and 14.25 for the southern equatorial Indian Ocean and progressive nutrient assimilation with a Redfield ratio of 16 ($\text{NO}_3^-/\text{PO}_4^{3-}$ -ass).

Page 20, line 16

RC: Is low temperature the only other possible explanation? Increasing numbers of reports are finding N_2 fixation at low temperature, thus the temperature limits seem to be a less convincing argument. What other contributing factors could be here?

AR: The sudden change in $\delta^{15}\text{N}$ and N^* is difficult to explain in the gyre as nutrients are not increasing. We have no data on micronutrients but find it unlikely that these change significantly within the gyre. Therefore, the only feasible explanation seems to be the temperature drop. However, we will stress the contradictory literature in the revised version.

Page 21, lines 10-11

RC: Can you make any connection here to the results of Martin and Casciotti, 2017 from the Arabian Sea?

AR: We will consider to add some sentences with respect to Martin and Casciotti (2017), but their work focuses on the Arabian Sea and not on the influence from the Arabian Sea on the south Indian Ocean.

Changes in the revised manuscript: “Nutrient distribution and nitrogen and oxygen isotopic composition of nitrate in water masses of the subtropical South Indian Ocean”

by Natalie C. Harms¹, Niko Lahajnar¹, Birgit Gaye¹, Tim Rixen^{1,2}, Kirstin Dähnke³, Markus Ankele³, Ulrich Schwarz-Schampera⁴ and Kay-Christian Emeis^{1,3}

¹Institute of Geology, Universität Hamburg, Hamburg, 20146, Germany.

²Leibniz-Centre for Tropical Marine Research, Bremen, 28359, Germany.

³Helmholtz-Zentrum Geesthacht (HZG), Institute for Coastal Research, Geesthacht, 21502, Germany.

⁴Federal Institute for Geosciences and Natural Resources (BGR), Hannover, 30655, Germany.

Pages and lines refer to the marked-up manuscript below.

Abstract

Page 1, line 10 - Page 2, line 8

We rewrote the Abstract in order to clarify our new findings (new nutrient and isotope data in a less explored ocean region accompanied by the first water mass distribution model in this ocean region) and added the depth range of the N* minimum. Furthermore, we added a sentence to the supply of newly fixed nitrogen in surface waters of the Indian Ocean subtropical gyre.

Introduction

Page 3, lines 2-3 and 5-6

We modified the sentences as Referee #1 suggested.

Page 3, lines 17-19

We modified the sentence.

Page 3, line 27

We added the reference Gruber and Sarmiento (1997).

Page 4, line 1-4

We added a paragraph to demonstrate the limitation of the tracer N*, and to strengthen the importance of using stable isotopes to overcome the weakness associated with the N* approach, following by the comments of Referee #1.

Page 4, lines 7-14

We shifted the formula for the δ -notation of nitrate $\delta^{15}\text{N}$ and $\delta^{18}\text{O}$ from the “Materials and Methods” section (Page 8, lines 30-31) to the “Introduction” section and added the definition of the isotope effect ϵ .

Page 4, lines 20-29:

We rewrote this paragraph to explain in more detail the benefit from the decoupling effect of N and O isotopes in nitrate regarding consumption and production processes. Additionally, we deleted tracer $\Delta(15,18)$ which is replaced by $\Delta(15-18)$ mentioned by Rafter et al., (2013) and is noted later in the manuscript.

Page 5, lines 11-13:

We added a sentence to note the lateral influence of preformed nutrients from the neighbouring ocean regions.

Materials and Methods

Page 6

We shifted Table 1 (CTD station list from the previous manuscript) to the supplement material.

Figure 1

To highlight the grey arrow that marks the South Equatorial Current (SEC), we added a black contour line to Figure 1.

Page 8, lines 22-23

We corrected the description of the measurement method of N and O isotopes, because we indeed use a two-point correction referred to IAEA and USGS standards.

Page 8, lines 30-31

We shifted the formula for the δ -notation of nitrate $\delta^{15}\text{N}$ and $\delta^{18}\text{O}$ from the “Materials and Methods” section to the “Introduction” section (Page 4, lines 7-9).

Results

Figure 2

In both Figures, 2a and 2b, black contour lines were changed into density surfaces, following the suggestion of Referee #2.

Figure 3

We added a temperature-salinity diagram, accompanied with oxygen concentrations, to demonstrate the clear difference of water masses in the southern and northern study area and to introduce Figure 5, presented later in the manuscript.

Page 10, line 10 - Page 11, line 6

We demonstrate more clearly the nutrient depleted surface layer and corrected the nutrient values mentioned in the density range of 24.9–26.4 kg/m³ (<300 m). Furthermore, we added the nutrient concentration in the depth range of the oxygen maximum ($\sigma = 26.4$ –26.9 kg/m³).

Figure 4 and Table 1 (revised manuscript)

We added Figure 4 to replace Tables 2 and 3 from the previous manuscript. These Tables are combined to one Table that now is Table 1 in the revised manuscript. Additionally, a column for water masses was added to get a better overview on the nutrient distribution and isotopic composition of nitrate in the individual water masses, which are explained in the following section. Therefore, we followed the suggestion of the Referee #1 and Referee #2.

Discussion

Page 14, lines 8-11

We added sentences to explain the development of the water mass distribution model by using the density-salinity and density-oxygen diagrams in Figure 5 and strengthen the importance of Figure 5.

Page 15, lines 5-11

We added more information on the Subantarctic Mode Water (SAMW) based on the study of Herraiz-Borreguero and Rintoul (2011), as suggested by the editor.

Page 15, line 11-13

We modified this sentence referred to the suggestion of Referee #1.

Page 15, line 17 and Page 16, line 5

We corrected the general density range of the boundary between intermediate and deep water masses.

Page 16, line 10-13

We modified the sentence to clarify that a further increase in oxygen as well as salinity at the 2°C level mark the transition from the Indian Deep Water (IDW) to the underlying Circumpolar Deep Water (CDW).

Page 20, line 1

We modified the subheading 4.2 as Referee #1 mentioned.

Page 20, lines 10-13

We added concrete values to demonstrate the increase in nutrient concentrations within the Indian Equatorial Water (IEW).

Figure 7

We added a latitudinal section (Figure 7g) to demonstrate the decoupling of N and O isotopes in our study area, especially within the Subantarctic Mode Water (SAMW) and the Red Sea-Persian Gulf Intermediate Water (RSPGIW). Therefore we used the tracer $\Delta(15-18)$ instead of $\Delta(15,18)$.

Page 23, line 7 and Page 31 line, 16

We removed the reference Bourbonnais et al. (2009), as required by Referee #1.

Page 23, lines 8-9

We added a sentence to the analytical error of N* values.

Figure 8

We corrected the colour-coding of the sample dots from “depth” to “density” and added the r^2 of the slope.

Page 25, lines 6-14

We rewrote this paragraph and added $\delta^{15}\text{N}$ values from the literature, detected in the Arabian Sea.

Page 25, line 15 - Page 26, line 12

We added a paragraph about the decoupling effect of N and O isotopes and the resulting elevated $\Delta(15-18)$ values in the Red Sea-Persian Gulf Intermediate Water (RSPGIW) and in the lower Indian Equatorial Water (IEW).

Page 26, lines 23-24

We rewrote these sentences and mentioned that also reduced iron availability could lead to partial N-assimilation in the Subantarctic region as well as light limitation.

Figure 9

In the previous manuscript, we removed Figure 7b, because we replaced tracer $\Delta(15,18)$ by tracer $\Delta(15-18)$ that is presented as latitudinal section in Figure 7g in the revised version. Additionally, we shifted Figure 8 from the previous manuscript to Figure 9 in the revised manuscript, which it is now Figure 9b. Furthermore, in Figure 9b, we changed the colour signatures for the different water masses consistently with the water mass classification in Figure 9a and added the Figure legend, following by the suggestions of Referee #2.

Page 30, line 9 - Page 31, line 8

We added sentences to the decoupling effect of N and O isotopes in Subantarctic Mode Water (SAMW) leading to lower $\Delta(15-18)$ values.

Page 31, line 15

We added the reference Gruber and Sarmiento (1997) and removed the reference to Bourbonnais et al. (2009), as required by both Referees.

Page 31, lines 17-23

Following by the suggestion of Referee #1, we rewrote this paragraph and added some information on the limitation of the N* approach and on atmospheric deposition and why we neglect this point in our further discussion.

Page 31 line 27 - Page 32, line 6

We rewrote this paragraph to make clear the increase of $\delta^{15}\text{N}$ values towards the surface layer (upper 200 m) compared to the underlying SAMW with strong elevated $\delta^{15}\text{N}$ values. We compared this upward increase accompanied with a lower $\Delta(15-18)$ in surface waters with studies in the NW Atlantic, indicating a similar upward increase, caused by N_2 -fixation.

Page 32, lines 23-24

We corrected the formula (2).

Page 33, line 4-14

We corrected the mean $\delta^{15}\text{N}$ of the SAMW (7.4 ‰ instead of 7.3 ‰). For the mean $\delta^{15}\text{N}$ of the surface water we take only into account the upper 200 m at latitude 20.36° S–23.91° S (5.0 ‰), which results in a calculated $\delta^{15}\text{N}-\text{NO}_3^-_{\text{new}}$ of ~4.9 ‰. We compared our results with the literature and backed our assumption of N_2 -fixation in surface waters of the ISOG at 20.36° S–23.91° S.

Figure 10

In Figure 10a, we modified colour and shape of the coloured dots that represent samples at latitudes 26.06° S–27.78° S, following by the comment of Referee #2. Additionally, instead of “ $\text{NO}_3^-_{\text{fix}}$ ” we named the supply of newly fixed nitrogen to the nitrate pool “ $\text{NO}_3^-_{\text{new}}$ ”. See also in the text at Page 32, line 29 - Page 33, line 11.

Page 35, lines 7-27

Following the suggestions of both Referees, we rewrote this paragraph and added the aspect of reduced iron availability as further explanation for the abrupt decline of N_2 -fixation south of ~26° S.

Conclusion

Page 36, lines 16-18

We adjusted this sentence according to the new tracer $\Delta(15-18)$.

Page 37, lines 2-9

We added information to the data availability of water column parameters, and nutrient and isotope data from research cruises MSM 59/2 in 2016 and SO 259 in 2017.

References

We adjusted the references according to our changes in the manuscript.

Nutrient distribution and nitrogen and oxygen isotopic composition of nitrate in water masses of the subtropical South Indian Ocean

Natalie C. Harms¹, Niko Lahajnar¹, Birgit Gaye¹, Tim Rixen^{1,2}, Kirstin Dähnke³, Markus Ankele³, Ulrich Schwarz-Schampera⁴ and Kay-Christian Emeis^{1,3}

¹Institute of Geology, Universität Hamburg, Hamburg, 20146, Germany.

²Leibniz-Centre for Tropical Marine Research, Bremen, 28359, Germany.

³Helmholtz-Zentrum Geesthacht (HZG), Institute for Coastal Research, Geesthacht, 21502, Germany.

⁴Federal Institute for Geosciences and Natural Resources (BGR), Hannover, 30655, Germany.

Correspondence to: Natalie C. Harms (natalie.harms@uni-hamburg.de)

Abstract. Vast subtropical gyres are important areas for the exchange of carbon between atmosphere and ocean in spite of low nutrient concentrations, and supposedly for the influx of reactive nitrogen to the ocean by dinitrogen fixation. To identify sources and transformation processes in the nitrogen cycle of the southern Indian Ocean subtropical gyre (IOSG) is one of five extensive subtropical gyres in the world's ocean. In contrast to those of the Atlantic and Pacific Ocean, the IOSG has been sparsely studied. In this study, we investigated the water mass distributions based on T/S and oxygen data, and concentrations of water column nutrients and stable isotope composition of nitrate of using waters samples from two expeditions in 2016 (MSM 59/2) and 2017 (SO 259) in the subtropical gyre, collected between ~30°S and the equator. Low nitrateOur results are the first in this ocean region and phosphate concentrations mark provide new information on the nutrient supply, and on sources and transformation processes in the nitrogen cycle. We identify the thick mixed-layer of nutrient depleted surface waters of the oligotrophic gyreIOSG with values of $5.93 \mu\text{M NO}_3^-$ and $0.53 \mu\text{M PO}_4^{3-}$ (340300 m; <math>\sigma_t < 26.4 \text{ kg/m}^3</math>). Increased nutrient concentrations towards the equator represent the northern endlimb of the gyre, characterized by typical strong horizontal gradients of the outcropping nutriclines. Measurements of stable isotopes of nitrate ($\delta^{15}\text{N}$ and $\delta^{18}\text{O}$) indicate isotopic maxima of $\delta^{15}\text{N} (> 7 \text{‰})$ and $\delta^{18}\text{O} (> 4 \text{‰})$ centred at 400–500 m, representing the preformed nitrate exportedThe influx of the Subantarctic Mode Water (SAMW) from the Southern Ocean injects oxygen saturated waters with mode water and induced by preformed nutrients, indicated by increased N and O isotope composition of nitrate ($\delta^{15}\text{N} > 7 \text{‰}$; $\delta^{18}\text{O} > 4 \text{‰}$) at 400–500 m (26.6–26.7 kg/m³), into the Subtropical thermocline. These values reflect partial N-assimilation there. Additionally, a in the Southern Ocean. Moreover, in the northern study area, a residue of nitrate affected by denitrification in the Arabian Sea is imported into the sub-thermoclineintermediate and deep water masses (>27.0 kg/m³) of the gyre, indicated by a strong N deficit (<math>N^* < -1 \text{ to } -4 \mu\text{M}</math>) within the northern study area, accompaniedand by elevated isotopic ratios of nitrate ($\delta^{15}\text{N} > 7 \text{‰}$; $\delta^{18}\text{O} > 3 \text{‰}$). The subtropical >7 ‰; $\delta^{18}\text{O} > 3 \text{‰}$). Remineralisation of partial-assimilated organic matter, produced in the Subantarctic, leads to a decoupling of N and O isotopes in nitrate and results in relatively low $\Delta(15-18)$ of <math>< 3 \text{‰}</math> within the SAMW. In contrast, remineralisation of ¹⁵N-enriched organic matter originated in the Arabian Sea indicates higher $\Delta(15-18)$ values of >4 ‰ within the Red Sea-Persian Gulf Intermediate Water (RSPGIW). Thus, the

subtropical South Indian Ocean is ~~thus~~ supplied by preformed nitrate from the lateral influx of water masses ~~that have similar isotopic character, but antagonistic origin (preformed versus regenerated). A from regions exhibiting distinctly different N-cycle processes documented in the dual isotope composition of nitrate. Additionally, a significant contribution of N₂-fixation within the Indian Ocean subtropical gyre (17° S–25° S) is promoted by~~ 23.91° S is inferred from reduced $\delta^{15}\text{N}$ values towards surface waters (upward decrease of $\delta^{15}\text{N}$ ~2.4 ‰), N* values of >2 μM and a relatively low nitrate-to-phosphate ratios in the surface layer, where approximately one-third (15–18) of <3 ‰. A mass and isotope budget implies that at least 34 % of the nitrate in the upper ocean is derived by between 20.36° S–23.91° S is provided from newly fixed N-nitrogen, whereas N₂-fixation appears to be limited by iron or temperature south of 26° S.

Formatiert: Schriftart: +Textkörper (Times New Roman)

Formatiert: Schriftart: +Textkörper (Times New Roman)

1 Introduction

The South Indian Ocean is dominated by a subtropical anticyclonic gyre (Gruber and Sarmiento and Gruber, 2006; Williams and Follows, 2003), the Indian Ocean Subtropical Gyre (IOSG), one of the major five subtropical gyres in the world's ocean. In contrast to those of the Atlantic and Pacific Oceans, where subtropical gyres occur north and south of the equator, the Indian Ocean developed only one subtropical gyre south of the equator. In comparison to the other subtropical gyres, the "Indian Ocean Subtropical Gyre" (IOSG) has been sparsely investigated. Between 10–20° S, the South Equatorial Current marks the northern limb of the IOSG (SEC; Duing, 1970; Pickard and Emery, 1982; Woodberry et al., 1989) and separates the subtropical gyre of the South Indian Ocean from the southern equatorial Indian Ocean. In the centre of the subtropical gyre, Ekman transport leads to an intensive downwelling (Williams and Follows, 1998), which results in a deepening of thermo-, pycno- and nutriclines. These layers shoal towards the fringe of the IOSG causing steep horizontal gradients (McClain et al., 2004).

Due to the intense downwelling and the resulting deepening of nutriclines, subtropical gyres form extensive oligotrophic regions, which occupy ~40 % of the Earth's surface (McClain et al., 2004). Since the biological productivity within these oligotrophic regions is relatively low and they are often referred to as "oceanic deserts" (Clark et al., 2008). However, due to their immense size they contribute significantly to atmosphere-ocean carbon fluxes (McClain et al., 2004).

Future global warming is assumed to strengthen stratification in low-latitude oceans and to expand the low productive subtropical gyres, accompanied by a decrease of the net primary production (Behrenfeld et al., 2006). This might have crucial impact on the marine nitrogen cycle. Therefore, to study the marine nitrogen cycle, we use nitrate and phosphate concentrations as well as the isotopic signature of nitrate are important indicators to study the marine nitrogen cycle (Deutsch et al., 2001; Deutsch et al., 2007; Gruber and Sarmiento, 1997; Lehmann et al., 2005; Sigman et al., 2005). The dominant source and sink of fixed, reactive nitrogen in the ocean are diazotrophic N₂-fixation and heterotrophic denitrification (Deutsch et al., 2001). N₂-fixation by diazotrophs, such as *Trichodesmium* is observed over much of the tropical and oligotrophic subtropical oceans (Karl et al., 1995; Michaels et al., 1996; Capone et al., 1997; Emerson et al., 2001). N₂-fixation compensating compensates the loss of reactive nitrogen during the heterotrophic denitrification if the ocean's marine nitrogen cycle is in a steady state (Deutsch et al., 2001).

The inputs of nitrogen (N) through N₂-fixation are unaccompanied by detached from inputs of phosphorus (P), leading to a decoupling of the nitrate (NO₃⁻) and phosphate (PO₄³⁻) pool. Deviations in the NO₃⁻ to PO₄³⁻ relationship from the Redfield-stoichiometry are used to study rates of both, N₂-fixation and denitrification (Gruber and Sarmiento, 1997; Sigman et al., 2005). Therefore, the tracer N* is used as an indicator for excesses and deficits in NO₃⁻ relative to the global NO₃⁻/PO₄³⁻ ratio and is expressed by the formula

$$N^* = [NO_3^-] - 16 \times [PO_4^{3-}] + 2.9 \mu\text{mol kg}^{-1} \quad (1)$$

$N^* = [NO_3^-] - 16 \times [PO_4^{3-}] + 2.9 \mu\text{M}$. The concept of N* has been discussed in detail by Gruber and Sarmiento (1997) and slightly modified by Deutsch et al. (2001). The concentration of 2.9 μM was added to bring the global mean of N* to about zero

(Gruber and Sarmiento and Gruber, 2006). However, the use of N* has limitations. First, the deviation from the Redfield stoichiometry may not always be a result of N inputs or outputs (N₂-fixation and denitrification) but may reflect also variations of uptake and remineralisation processes (Sigman et al., 2005). Second, input and losses partially overprint each other when they occur simultaneously in the same water body.

- 5 We use stable isotopes of nitrate (N and O) to overcome the weakness associated with the N* approach and distinguish between sources and sinks of fixed nitrogen and to study transfer processes in the nitrogen cycle (e.g., N₂-fixation, N-assimilation, denitrification, N-assimilation-nitrification, N₂-fixation), also when they occur simultaneously. Isotope ratios are reported in ‰ using the δ-notation ($\delta^{15}\text{N} = [({}^{15}\text{N}/{}^{14}\text{N}_{\text{sample}})/({}^{15}\text{N}/{}^{14}\text{N}_{\text{atm.N}_2})] - 1 \times 1000$; $\delta^{18}\text{O} = [({}^{18}\text{O}/{}^{16}\text{O}_{\text{sample}})/({}^{18}\text{O}/{}^{16}\text{O}_{\text{VSMOW}})] - 1 \times 1000$, with air N₂ and VSMOW as reference for ¹⁵N/¹⁴N and ¹⁸O/¹⁶O, respectively). During consumption processes of nitrate, e.g., N-assimilation or denitrification, heavier/lighter isotopes (¹⁵N and ¹⁸O) are preferentially assimilated, leaving the substrate enriched in the residual nitrate pool, leading ¹⁵N and ¹⁸O according to elevated δ¹⁵N and δ¹⁸O values. The difference between the isotopic ratio of the substrate (dissolved nitrate) and the product (organic N) defines the isotopic fractionation factor ε in permil (Mariotti et al., 1981); its isotope effect (¹⁵ε and ¹⁸ε, e.g., ¹⁵ε is defined as ¹⁴k/¹⁵k-1, where ¹⁴k and ¹⁵k are the rate coefficients of the reactions for the ¹⁴N- and ¹⁵N-bearing forms of nitrate). Several culture experiments indicate a ¹⁵ε: ¹⁸ε-1 during denitrification and N-assimilation typical for processing of preformed nitrate (Granger et al., 2004; Sigman et al., 2003; Sigman et al., 2005). In contrast, nitrification that δ¹⁵N and δ¹⁸O of biomass originating from N₂ fixation decouples N and O isotopes in nitrate pools with a significant contribution of newly fixed N. The net balance between the residual nitrate pool rise equally as consumption proceeds, consequently the O-to-N isotope effect (¹⁸ε: ¹⁵ε) is close to 1 (Granger et al., 2004; Rafter et al., 2013; Sigman et al., 2003; Sigman et al., 2005).
- 20 While nitrate consumption processes such as N-assimilation and denitrification and lead to indistinguishable imprints on N and O isotope compositions, nitrate production (N₂-fixation or processes (nitrification) is expressed by the tracer Δ(15,18) (and N₂-fixation) have very different effects on the N and O isotopes of nitrate (Rafter et al., 2013; Sigman et al., 2005). Whereas almost all of the ammonium generated from organic N is oxidized to nitrate in oxic subsurface waters of the open ocean, the N isotope effect associated with ammonium production and nitrification do not affect the δ¹⁵N-NO₃⁻. Therefore, the N isotope effect depends more on the biomass being remineralised (Rafter et al., 2013; Sigman et al., 2005). In contrast, the δ¹⁸O of newly nitrified nitrate is independent of the isotopic composition of the organic matter and leads to a counteracting behaviour of δ¹⁵N and δ¹⁸O. Consequently, the decoupling of N and O isotopes provide a better understanding of nitrate assimilation and regeneration processes in marine environments (Casciotti et al., 2008; DiFiore et al., 2009; Sigman et al., 2005, 2009, Wankel et al., 2007).

$$30 \Delta(15,18) = (\delta^{15}\text{N} - \delta^{15}\text{N}_{\text{deep}}) - \frac{15}{18} \epsilon_{\text{N}} \epsilon_{\text{O}} \times (\delta^{18}\text{O} - \delta^{18}\text{O}_{\text{deep}}) \quad (2)$$

The δ¹⁵N_{deep} and δ¹⁸O_{deep} are the mean of water masses, which are taken to approximate the source of nitrate to the upper water column.

Our investigations in the South Indian Ocean are part of environmental studies in the INDEX (Indian Ocean Exploration) program for marine resource exploration by the federal Institute for Geosciences and Natural Resources (BGR), Germany, and the International Seabed Authority (ISA). We use CTD measurements and analyse seawater samples to determine nutrient concentrations and stable isotopes of nitrate ($\delta^{15}\text{N}$ and $\delta^{18}\text{O}$) along a transect from the IOSG to the southern equatorial Indian

5 Ocean. The main goal of this study is to investigate the relatively unknown hydrology and the unexplored distribution of nutrients and stable isotopes of nitrate along a transect from to identify N-cycle processes within the IOSG towards the southern-equatorial South Indian Ocean. Therefore, we use CTD measurements and analyse seawater samples to determine nutrient concentrations and stable isotopes of nitrate ($\delta^{15}\text{N}$ and $\delta^{18}\text{O}$). First, we identify the water masses and their provenance by their unique characteristic physical properties and demonstrate their influence on establish the nutrient first water mass
10 distribution and isotopic composition of water column nitrate model for this ocean region. In a second step, we use new nutrient and stable isotope data to determine nutrient sources to the IOSG and their role in the global marine nitrogen cycle. Furthermore, we demonstrate the influence of water masses on the nutrient distribution and the isotopic composition of water column nitrate by the influx of preformed nutrients. Our results of nutrient and isotope measurements are the first in the IOSG and bridge the gap between several investigations in the Arabian Sea (e.g., Brandes et al., 1998; Gaye-Haake et al., 2005; Gaye et al., ~~2005~~;
15 Gaye et al., 2013; Ward et al., 2009) and in the Southern Ocean (e.g., Bianchi et al., 1997; DiFiore et al., 2006; DiFiore et al., 2010; Sigman et al., 1999, 2000).

2 Materials and Methods

2.1 CTD measurement and sample collection

In total, 313 seawater samples were collected at 15 CTD stations (Table 1; Fig. 1) during two expeditions with R/V Maria S.
20 Merian (MSM 59/2 “INDEX 2016-2”; November–December 2016) and R/V Sonne (SO 259 “INDEX 2017”; August–October 2017). The CTD was equipped with sensors to determine density, temperature, salinity and oxygen at overall 17 CTD stations from the surface down to the sea floor. No water samples were collected at stations 07 and 11.

The study area covers the region of the IOSG from 30°S, across the SEC at 10–20°S and towards the equator. Fourteen CTD stations (Table 1; Fig. 1) are located within the IOSG from 20.36° S to 27.78° S and 67.07° E to 73.92° E. CTD 05 is located
25 in the region of the SEC (15.08° S, 74.05° E) and at the northern end of the IOSG. The northernmost CTD stations (CTD 01, 03; 2017) at 8.81°S 75.67°E and 2.98°S 77.16°E are positioned in the southern equatorial Indian Ocean, north of the SEC. Seawater samples were collected for measurements of nutrients and stable isotopes of nitrate. Samples were filtered through a nucleopore Nucleopore polycarbonate filter (0.454 μm) with a metal- and silicon-free Nalgene filtration unit. The filtered water was bottled in Falcon PE tubes (45 ml) and immediately stored at -20°C during the cruise. The samples were shipped as frozen
30 airfreight (-20°C) to Germany. Nutrient concentrations and stable isotopes of nitrate (N and O) were determined in the home lab immediately after arrival in the home lab.

Table 1: Location of CTD stations during cruises MSM 59/2 (INDEX 2016) and SO 259 (INDEX 2017).

CTD station	Latitude [°S]	Longitude [°E]
Cruise MSM 59/2 in 2016		
03	23.01	67.07
14	23.87	69.50
22	22.89	69.16
32	21.78	69.02
35	21.61	69.44
52	21.17	68.62
67	21.72	67.67
Cruise SO 259 in 2017		
01	2.98	77.16
03	8.81	75.67
05	15.08	74.05
07	20.36	69.75
11	20.67	69.32
15	20.96	68.92
45	23.91	69.56
49	26.05	70.84
60	27.78	73.92
99	27.01	72.40

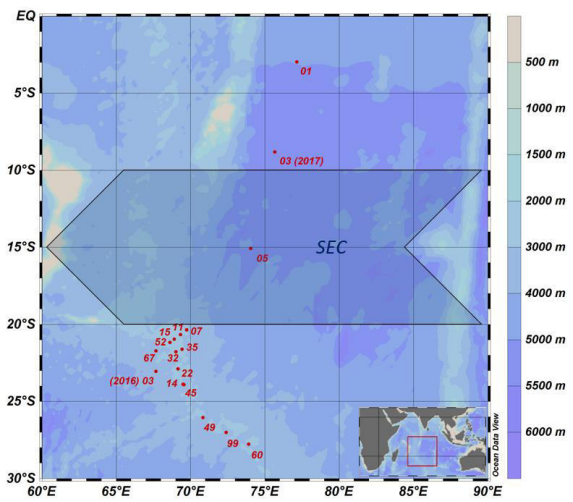
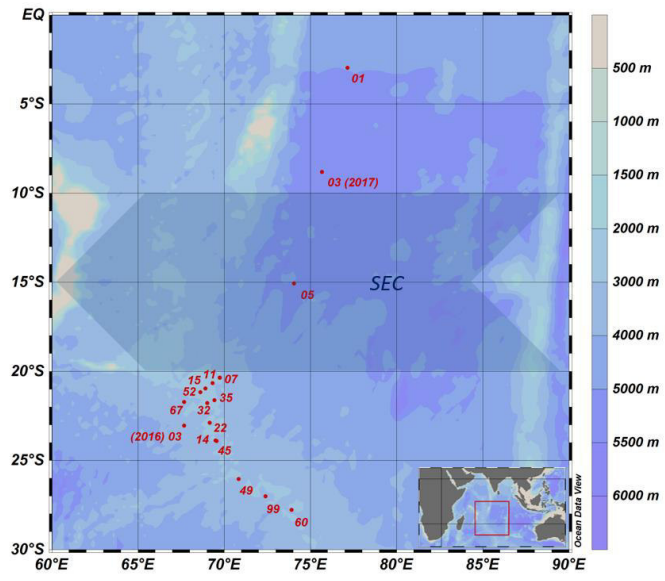


Figure 1: Sampling location during the cruises MSM 59/2 (INDEX 2016-2) and SO 259 (INDEX 2017). Shaded arrow represents the westward-directed, broad South Equatorial Current (SEC) after Woodberry (1989) from 10–20°S. Colors/Colours denote water depths.

2.2 Nutrient analyses

Nutrient concentrations (NO_x , NO_2^- , NH_4^+ , PO_4^{3-}) were measured with a SEAL AutoAnalyzer3HR with standard colorimetric/colorimetric methods (Grasshoff et al., 2009). Ammonia and nitrite concentrations were below detection limit. Nitrate determination included reduction of nitrate to nitrite with a cadmium reduction column. Nitrite ions reacted with sulphanilamide to form a diazo compound, followed by a reaction to an azo dye with N-(1-naphtyl)-ethylenediamine (NEDD) and was measured at 520–560 nm. Phosphate determination followed the method of Murphy and Riley (1962). Under acid conditions a phosphomolybdic complex was formed of ortho-phosphate, antimony and molybdate ion (Wurl, 2009). Followed by reduction of ascorbic acid, the blue color/color complex was measured at 880 nm. The relative error of duplicate sample measurements was below 1.5 % for nitrate and phosphate concentrations and detection limit was $<0.5 \mu\text{M}$ for NO_x and $>0.1 \mu\text{M}$ for PO_4^{3-} .

2.3 Measurements of N and O isotopes of nitrate

Isotope measurements were only conducted for samples with nitrate concentrations $>1.7 \mu\text{M}$. Stable isotopes of nitrate ($\delta^{15}\text{N}$ and $\delta^{18}\text{O}$) were determined using the “denitrifier” method (Casciotti et al., 2002; Sigman and Casciotti, 2001). Nitrate was converted to N_2O gas using denitrifying bacteria (*Pseudomonas aureofaciens*). Based on nitrate concentrations, sample volumes were adjusted to yield 10 nmoles N_2O and were injected into suspensions of *Pseudomonas aureofaciens* (ATCC#13985) for combined analysis of $\delta^{15}\text{N}$ and $\delta^{18}\text{O}$. The resulting N_2O gas in headspace was purged into a GasBench II (ThermoFinnigan), and analysed in a Delta V Advantage and a Delta V Plus mass spectrometer. The results were calibrated using IAEA-N3 ($\delta^{15}\text{N}\text{-NO}_3^- = +4.7 \text{‰}$ and $\delta^{18}\text{O}\text{-NO}_3^- = +25.6 \text{‰}$) and USGS-34 ($\delta^{15}\text{N}\text{-NO}_3^- = -1.8 \text{‰}$ and $\delta^{18}\text{O}\text{-NO}_3^- = -27.9 \text{‰}$) (Böhlke et al., 2003). A further internal potassium nitrate standard was analysed within each run for quality assurance. Isotope values were corrected using the “bracketing scheme” from Nitrate and nitrite are Sigman et al. (2009) for $\delta^{18}\text{O}\text{-NO}_3^-$ and a two-point correction referred to IAEA-N3 and USGS-34 for $\delta^{15}\text{N}\text{-NO}_3^-$ and $\delta^{18}\text{O}\text{-NO}_3^-$. The standard deviation for IAEA-N3 was better than 0.2 ‰ for $\delta^{15}\text{N}\text{-NO}_3^-$ and 0.3 ‰ for $\delta^{18}\text{O}\text{-NO}_3^-$, which is within the same specification for $\delta^{15}\text{N}\text{-NO}_3^-$ and $\delta^{18}\text{O}\text{-NO}_3^-$ for at least duplicate measurements of the samples, converted to N_2O gas using denitrifying bacteria (*Pseudomonas aureofaciens*). Based on nitrate concentrations, sample volumes were adjusted to yield 10 nmoles N_2O and were injected into suspensions of *Pseudomonas aureofaciens* (ATCC#13985) for combined analysis of $\delta^{15}\text{N}$ and $\delta^{18}\text{O}$. The resulting N_2O gas in headspace was purged into a GasBench II (ThermoFinnigan), and analysed in a Delta Plus XP mass spectrometer. Isotope ratios are reported in ‰ using the δ notation:

$$\delta^{15}\text{N} = \left[\frac{(^{15}\text{N}/^{14}\text{N})_{\text{sample}}}{(^{15}\text{N}/^{14}\text{N})_{\text{atm. N}_2}} - 1 \right] \times 1000 \quad (3)$$

$$\delta^{18}\text{O} = \left[\frac{(^{18}\text{O}/^{16}\text{O})_{\text{sample}}}{(^{18}\text{O}/^{16}\text{O})_{\text{VSMOW}}} - 1 \right] \times 1000 \quad (4)$$

Formatiert: Tiefgestellt

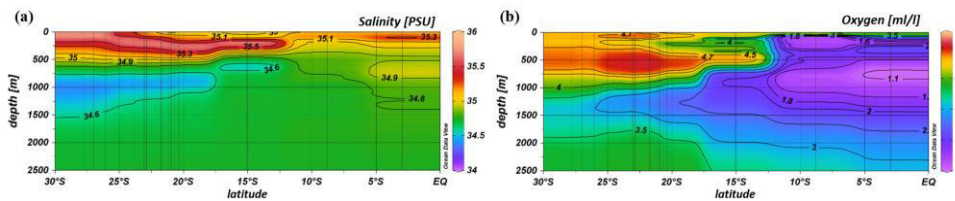
Formatiert: Tiefgestellt

with air N_2 and VSMOW as reference for $^{15}N/^{14}N$ and $^{18}O/^{16}O$, respectively. The values were calibrated using IAEA-N3 ($\delta^{15}N-NO_3^- = +4.7\text{‰}$ and $\delta^{18}O-NO_3^- = +25.6\text{‰}$) and USGS 34 ($\delta^{15}N-NO_3^- = -1.8\text{‰}$ and $\delta^{18}O-NO_3^- = -27.9\text{‰}$) (Böhlke et al., 2003). A further internal potassium nitrate standard was analysed within each run for quality assurance. Isotope values were corrected using the “bracketing scheme” from Sigman et al. (2009) for $\delta^{18}O-NO_3^-$ and the single point correction referred to IAEA-N3 for $\delta^{15}N-NO_3^-$. The standard deviation for IAEA-N3 was 0.2‰ for $\delta^{15}N-NO_3^-$ and 0.3‰ for $\delta^{18}O-NO_3^-$, which is within the same specification for $\delta^{15}N-NO_3^-$ and $\delta^{18}O-NO_3^-$ for at least duplicate measurements of the samples.

3 Results

3.1 Physical water column properties

South of 25° S the upper 170 m are characterized by an intense salinity maximum with values of >35.5 PSU (Fig. 2a) and temperatures above 15°C (Figs. 2a, 3). The salinity maximum is carried northwards and is subducted underneath the surface layer within a temperature range of 22–15°C and with a core density of $\sigma=25.5\text{ kg/m}^3$ (~250 m). Further north (CTD 03, 2017; 8.81° S) at the same density level, the salinity is significantly lower and reveals values of 35.2 PSU. The northernmost station (CTD 01, 2017; 2.89°S) indicates again a slight increase in salinity (>35.3 PSU). Between 22° S and 10° S, less saline surface water (<35.1 PSU) lies above the density level of the salinity maximum with temperatures of >23°C and densities above 24.0 kg/m^3 (<150 m). South of 15° S, directly underneath the salinity maximum an oxygen maximum with values of >4.7 ml/l occurs at a density range of 26.4–26.9 kg/m^3 (250–750 m; Fig. 2b) and temperatures between 8°C and 15°C and 8°C (Fig. 3). The lower limit of the oxygen maximum coincides with a temperature level of 8–9°C at $\sigma=26.9$ –27.0 kg/m^3 and marks the permanent thermocline at a depth of ~750 m in the south and at a depth of ~500 m in the north. Oxygen concentrations decrease towards the north and fall below 2 ml/l at the northernmost stations (CTD 01, CTD 03; 2017; Figs. 2b, 3). Below the permanent thermocline (<9°C), an absolute salinity minimum with values less than 34.6 PSU is found in the southern region (Figs. 2a, 3), within a density range of 26.9–27.4 kg/m^3 (core density $\sigma=27.2\text{ kg/m}^3$), which is strongly diluted further north. In the southern equatorial Indian Ocean at CTD 01, an increase in salinity (>34.9 PSU; $\sigma=27.2\text{ kg/m}^3$) corresponds with reduced oxygen concentrations of <1.1 ml/l. Overall, low oxygen concentrations dominate the northern study area and extend to the sub-thermocline deeper water masses at the southernmost stations (<3.5 ml/l; Figs. 2b, 3).



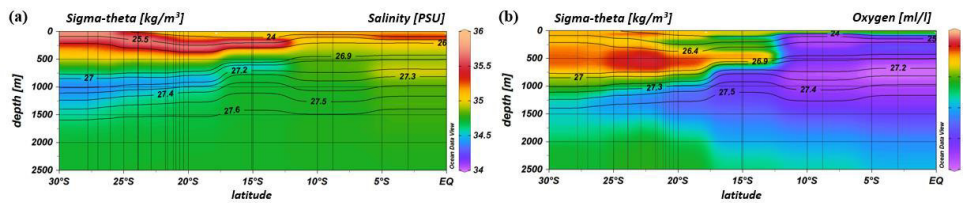


Figure 2: Profiles of salinity (a) and oxygen distribution (b) from CTD measurements during cruises MSM 59/2 (2016) and SO 259 (2017). Contour lines indicate the potential density sigma-theta in kg/m³.

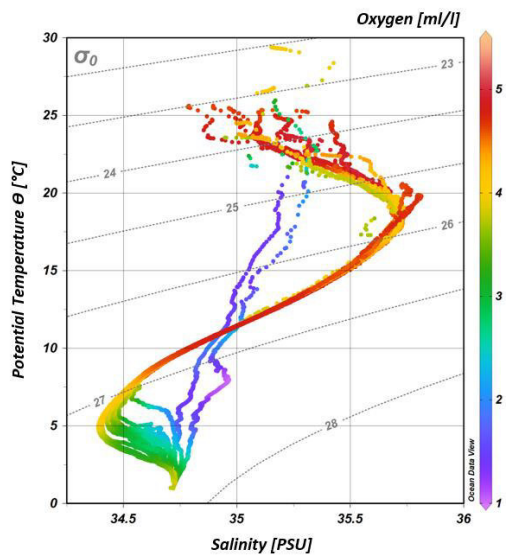


Figure 3: T-S diagram (potential temperature vs. salinity) from CTD measurements during cruises MSM 59/2 (2016) and SO 259 (2017). The colour bar indicates oxygen concentrations and grey, dotted lines represent density surfaces in sigma-theta (kg/m³). The northernmost CTD stations (CTD 01, CTD 03; 2017) are characterized by low oxygen concentrations (<2 ml/l) and less variations in the salinity distribution, while the water column profiles in the IOSG indicate a distinct salinity maximum and minimum, respectively.

3.2 Nutrient concentration

- 10 The upper water column, in the depth range of the salinity maximum south of 20° S (<26.4 kg/m³), is within the subtropical gyre. The upper 100 m are strongly depleted in nitrate (~5.9 μM) and phosphate (<0.5 μM; Table 2), with concentrations less

Formatiert: Abstand Vor: 18 Pt.

than 1 μM of nitrate and less than 0.1 μM of phosphate (Fig. 4a, 4b; Table 1). Within the depth range of the salinity maximum (24.9–26.4 kg/m^3 ; <300 m), nutrient concentrations are still minor with values of <3 μM NO_3^- and <0.3 μM PO_4^{3-} (Table 1). Nutrient concentrations rise within the depth range of the oxygen maximum ($\sigma = 26.4$ –26.9 kg/m^3), where the nutrient we observe concentrations of ~11 μM NO_3^- and <0.9 μM PO_4^{3-} before they reach values up to ~21 μM for nitrate and 1.5 μM for phosphate. Within the intermediate waters (~1000 m), nitrate and phosphate concentrations attain typical deep-sea values of >30 μM and >2 μM (Gruber and Sarmiento and Gruber, 2006) within intermediate waters (>26.9 kg/m^3 ; >750 m). Across the northern fringe of the gyre, at surface waters, (CTD 05 (2017; 15.08° S)) nutrient concentrations slightly increase (Table 2) (Figs. 4a, 4b).

Further north, at stations CTD 01 and 03 (2.98–8.81° S), nutrient concentrations in the upper water column reach values typical for open ocean areas that are unaffected by gyral downwelling or high biological production (Figs. 4a, 4b). At 90 m water depth, concentrations were ~11 μM for nitrate and ~1 μM for phosphate (Table 2). Within the thermocline (<23.0–27.0 kg/m^3 ; <550 m), nutrient concentrations attain values of >28.2 μM for nitrate and >2.7 μM for phosphate, before they level out at values of >35 μM for nitrate and >2.5 μM for phosphate at greater depth (Table 1).

Table 2: Nitrate and phosphate concentrations summarized for CTD stations within the subtropical gyre (27.78°S–20.96°S), at the northern fringe (15.08°S) and north of the gyre (8.81°S–2.98°S). Samples were collected during cruises MSM 59/2 (INDEX 2016-2) and SO 259 (INDEX 2017). Results in the same area are similar and shown together.

Latitude [°S]	Sigma-theta [kg/m^3]	Depth [m]	NO_3^- [μM]	PO_4^{3-} [μM]
27.78–20.96	26.4	310	5.9	0.5
	26.9	770	21.2	1.5
	27.4	1210	31.6	2.3
15.08	26.6	300	7.7	0.5
	26.9	550	22.7	1.6
	27.4	900	36.0	2.6
8.81–2.98	24.0	90	11.1	0.8
	27.0	550	28.2	2.0
	27.3	850	38.0	2.7

3.3 N and O isotopes of nitrate

In the upper 700 m–750 m (<26.9 kg/m^3), distinct N and O isotope maxima with $\delta^{15}\text{N}$ of >7.0 ‰ and $\delta^{18}\text{O}$ of >4.0 ‰ are found at latitudes 27.78° S–15.08° S (Table 3). This maximum is centred at (Table 1; Figs. 4c, 4d). N and O isotope maxima are observed at ~400–500 m (26.6–26.7 kg/m^3) and correlates with the oxygen maximum of >4.7 ml/l. Between latitudes 23.91° S and 20.96° S, the N isotope maximum is observed at 400 m and, whereas the O isotope maximum is observed at 500 m, so that the. Consequently, N and O isotope maxima are indicating an offset by of ~100 m (Table 3) (see supplement tables S2 and S3). Above the isotopic maximum, both $\delta^{15}\text{N}$ and $\delta^{18}\text{O}$ decrease to values of ~5.4 ‰ and

Formatiert: Englisch (Vereinigtes Königreich)

Formatiert: Abstand Nach: 0 Pt.

Formatiert: Schriftart: 10 Pt.

Formatiert: Abstand Vor: 18 Pt.

Formatiert: Schriftfarbe: Text 1

Formatiert: Schriftfarbe: Text 1

Formatiert: Schriftfarbe: Text 1

Formatiert: Schriftfarbe: Text 1

Formatiert: Schriftfarbe: Text 1

~2.1 ‰, respectively, in the upper 300 m; an exception are the southernmost stations (CTD 49, 60, 99; 2017), where the elevated isotope $\delta^{15}\text{N}$ values extend up to the surface:

(Fig. 4c). In surface waters further north (<250 m), $\delta^{15}\text{N}$ and $\delta^{18}\text{O}$ increase to values of >7.0 ‰ and >4 ‰, respectively, at the northernmost station (CTD 01, 2017; Figs. 4c, 4d). Underneath this surface layer, N and O isotope ratios slightly decrease at ~180 m, before $\delta^{15}\text{N}$ and $\delta^{18}\text{O}$ again rise to >7.0 ‰ and >3.0 ‰, with an extended maximum in the depth interval from 300 m to 900 m (<27.3 kg/m³) that coincides with elevated salinities. Below the isotopic maxima in the southern region at ~400–500 m, and below the depth interval with high δ -values in the northernmost CTD station, $\delta^{15}\text{N}$ and $\delta^{18}\text{O}$ decrease towards deeper waters and have average values of 5.8 ‰ and 2.3 ‰ (Table 3) (Figs. 4c, 4d).

Table 3: Average isotopic composition

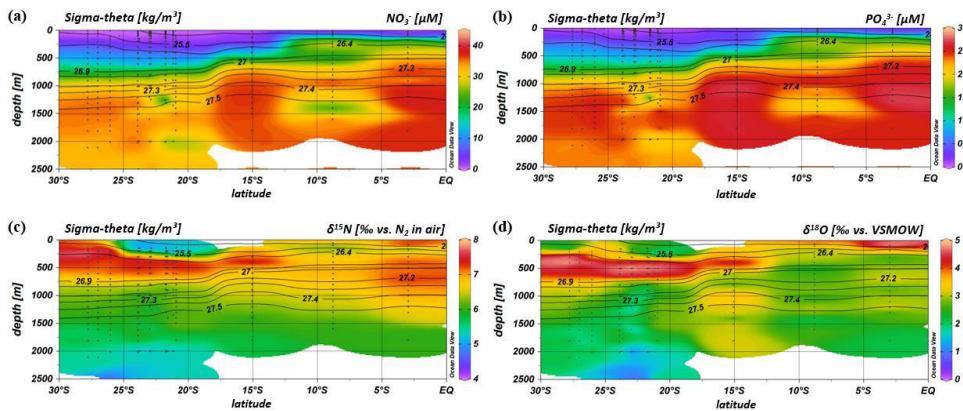


Figure 4: Profiles of nitrate in the surface layer, within the thermocline (a) and in intermediate phosphate concentrations (b) and deep waters of all CTD stations $\delta^{15}\text{N}$ (c) and $\delta^{18}\text{O}$ (d) of seawater samples collected during cruises MSM 59/2 (INDEX 2016-2) and SO 259 (INDEX 2017). Data are combined for latitude. Contour lines indicate the potential density sigma-theta in kg/m³.

Table 1: Average nitrate and phosphate concentrations and average $\delta^{15}\text{N}$ and $\delta^{18}\text{O}$ values within water masses of the South Indian Ocean, defined along their potential density surfaces (sigma-theta) and separated into four latitudinal sections (2.98–8.81° S, 27.78–26.05 °S; 23.91–20.36 °S; 15.08° S, 20.96–23.91° S and 26.05–27.78°; 8.81–2.98 °S) that have similar isotopic composition. ^a $\delta^{15}\text{N}$ and $\delta^{18}\text{O}$ maxima. ^b Water depth of isotopic maxima. Results in the same area and shown together. Water mass abbreviations as followed: Indonesian Upper Water (IUW), Subantarctic Surface Water (SSW), Subantarctic Mode Water (SAMW), Indian Equatorial Water (IEW).

Formatiert: Englisch (Vereinigtes Königreich)

Formatiert: Abstand Nach: 0 Pt.

Formatiert: Schriftart: +Textkörper (Times New Roman)

Formatiert: Schriftart: +Textkörper (Times New Roman)

Formatiert: Abstand Nach: 0 Pt.

Antarctic Intermediate Water (AAIW), Indonesian Intermediate Water (IIW), Red Sea-Persian Gulf Intermediate Water (RSPGIW), Indian Deep Water (IDW), and Circumpolar Deep Water (CDW).

Latitude [°S]	Depth [kg/m ³] {Sigma-theta}	Water masses	NO ₃ ⁻ [μM ± 1 D.A.]	PO ₄ ³⁻ [μM ± 1 D.A.]	δ ¹⁵ N [‰] NO ₃ ⁻ [‰ ± 1 D.A.] ^a	δ ¹⁸ O [‰] NO ₃ ⁻ [‰ ± 1 D.A.] ^b
27.78-26.05	<26.4	SSW	1.67 ± 0.24 ± 0.15	1.59 ± 0.24 ± 0.15	7.62 ± 0.30	2.94 ± 0.47
	<700	SAMW	11.43 ± 5.0	4.40 ± 3.70	7.25 ± 0.31	4.34 ± 0.52
	26.9					
	26.9-27.78	800-1200 AAIW	28.71 ± 5.24 ± 2.05 ± 0.32	2.05 ± 0.32	6.328 ± 0.16	3.295 ± 0.40
	26.05					
	1300	5.7 Deep Water Masses	34.55 ± 1.02 ± 2.248 ± 0.07	2.248 ± 0.07	5.68 ± 0.29	2.17 ± 0.26
	>3000	>27.4				
23.91-20.36	<24.9	Surface Water/IUW	0.37 ± 0.26 ± 0.08 ± 0.03	0.08 ± 0.03	N/D	N/D
	<300	524.9-26.4 SSW	2.485 ± 0.98 ± 11.04 ± 2.76 ± 0.29 ± 0.08	0.29 ± 0.08	5.41 ± 0.54	2.07 ± 0.44
	300	7.3 SAMW			7.7 ± 0.25 ± 4.00 ± 0.35 ± 0.29	4.560 ± 5.0 ± 0.29 ± 0.29
	650					
	26.9-27.4	AAIW	28.57 ± 3.23 ± 20.96 ± 0.23 ± 32.72 ± 2.54 ± 2.34 ± 0.16	800 ± 1000 ± 1.99 ± 0.13 ± 0.32	6.222 ± 0.13 ± 0.32	2.421 ± 0.32
	1500	Deep Water Masses			5.545 ± 0.30 ± 1.662 ± 0.32	
	>3000	>27.4				
15.08	<24.3	IUW	1.69 ± 1.15 ± 4.42 ± 3.27 ± 7.15 ± 1.11 ± 1.16	0.30 ± 0.06	N/D	N/D
	24.3-26.6	SSW			N/D	N/D
	<500	26.6-26.9 SAMW			7.6 ± 0.26 ± 4.01 ± 4.6 ± 0.40 ± 0.40	
	600	AAIW/IIW	30.74 ± 3.30 ± 2.18 ± 0.26	6.668 ± 0.05 ± 2.894 ± 0.08		
	800	26.9-27.2 Deep Water Masses			6.06 ± 0.49 ± 3.403 ± 0.45	
	900					
	>5000	>27.2				
			8.5	7.3		4.9
8.81-2.98	400-250	Surface Water	0.61 ± 0.26 ± 0.17 ± 0.04	0.17 ± 0.04	6.366 ± 0.41 ± 3.377 ± 0.55	
	23.0-27.0	IIW	22.84 ± 5.85 ± 32.77 ± 3.23 ± 1.57 ± 0.34	1.57 ± 0.34	6.96 ± 0.07	2.86 ± 0.14
	27.0-27.3	RSPGIW			7.03 ± 0.67 ± 5.909 ± 0.09	2.8 ± 2.7

Eingefügte Zellen

Formatiert

Eingefügte Zellen

Eingefügte Zellen

Formatiert

Formatiert

Formatiert

Formatiert

Formatiert

Formatiert

Formatiert

Formatierte Tabelle

Formatiert

Formatiert

Formatiert

Gelöschte Zellen

Eingefügte Zellen

Formatiert

Formatiert

Formatiert

Eingefügte Zellen

Formatiert

Gelöschte Zellen

Formatiert

Gelöschte Zellen

Eingefügte Zellen

Formatiert

Eingefügte Zellen

Eingefügte Zellen

Formatiert

Formatiert

Formatiert

Formatiert

Formatiert

Formatiert

Formatiert

Formatiert

Eingefügte Zellen

Formatiert

Formatiert

Formatiert

Formatiert

Formatiert

Formatiert

Eingefügte Zellen

Formatiert

			35 ± 0.19	1250 >5000		2.485 ± 0.23
27.3–27.7	IDW	$\frac{34.21 \pm 4.59}{4.59}$	2.48 ± 0.23		6.56 ± 0.19	2.72 ± 0.36
>27.7	CDW	$\frac{35.92 \pm 0.48}{0.48}$	2.41 ± 0.05		5.32 ± 0.24	2.07 ± 0.13

^a $\delta^{15}\text{N-NO}_3^-$ in ‰ versus air and ^b $\delta^{18}\text{O-NO}_3^-$ in ‰ versus VSMOW; D.A. = deviation from the average value; N/D = not detectable due to insufficient nitrate concentrations.

4 Discussion

5 4.1 Water mass distribution

Water masses in the workingstudy area are well discernible by their densities, salinities and oxygen concentrations (Fig. 35). In accordance with definitions from the literature, we identified water masses from the IOSG towards the southern equatorial Indian Ocean and established the first water mass distribution model for this ocean region (Fig. 6). To generate the water mass distribution model, we use salinity and oxygen distributions along sigma-theta surfaces. We separate our study area in three latitudinal sections, which demonstrate the alteration of water masses along the latitudinal transect and between the different ocean regimes (Fig. 5). We present the provenance of water masses of Antarctic and Subantarctic origin converging and mixing with water masses from the southern equatorial Indian Ocean and the Arabian Sea. The water mass distribution model is depicted in Fig. 4, which serves as a basis for the understanding of our nutrient and coupled N and O isotope measurements of nitrate.

15 4.1.1 Surface and thermocline waters (<26.9 kg/m³; <800 m)

A high salinity surface layer (>35.5 PSU) centred at ~25.45 kg/m³ (Fig. 3a5a) is described in several studies. It has been termed “southern subtropical surface water” by Muromtsev (1959), “subtropical surface water” by Wyrтки (1973) and “subtropical subsurface water” (SSW) by Schott and McCreary (2001). For further descriptions, we adopt the definition of Wyrтки (1973) and use the abbreviation SSW. The SSW is formed in the subtropical gyre of the southern hemisphere by excess of evaporation over precipitation (Schott and McCreary, 2001) at latitudes 25–35° S (Baumgartner and Reichel, 1975). It is subducted into the thermocline of the subtropical gyre (Schott and McCreary, 2001), is detectable as far north as 15.08° S at CTD 05 (Fig. 3b) and not discernable further north in the southern equatorial Indian Ocean (Figs. 3c, 45c, 6).

20 Less saline surface water (<35.1 PSU) occurs above the density level of the salinity maximum (>23°C; <24.0 kg/m³; Fig. 3b5b) and is described by Wyrтки (1971) and Warren (1981). These low salinity values reflect an excess of precipitation over evaporation at latitudes 0–10° S (Baumgartner and Reichel, 1975) accompanied by the influx of low salinity water (34.0–34.5 PSU) from the Pacific Ocean through the Indonesian Archipelago, called “Indonesian Throughflow” (ITF). The

Formatiert: Schriftart: 9 Pt.

Formatiert: Block

Formatiert: Block

Formatiert: Schriftart: 9 Pt.

Formatiert: Abstand Vor: 18 Pt.

ITF carries less saline water westwards by the SEC within the entire thermocline (Wyrcki, 1971; You and Tomczak, 1993). Emery (2001) named this less saline surface water (34.4–35.0 PSU) “Indonesian Upper Water” (IUW; Fig. 46).

The oxygen maximum south of 20° S in a density range of 26.4–26.9 kg/m³ (250–750 m; Fig. 3d5d) corresponds with the “Subantarctic Mode Water” (SAMW; Figs. 3, 45, 6), described by McCartney (1977). It is formed at latitudes 40° S–50° S and injects oxygen saturated waters at a temperature range of 6–14°C into the subtropical gyre. The SAMW in the South Indian Ocean can be separated into three modes by slightly different density distributions (Herraiz-Borreguero and Rintoul, 2011) which are originated in different ocean regions. For example, a lighter mode of the SAMW is formed in the western Indian basins and is limited to the southwest portion of the subtropical gyre, while the denser mode is found south off Australia and is carried further north by the outer portion of the subtropical gyre and ventilate a larger fraction of the gyre interior (Herraiz-Borreguero and Rintoul, 2011). However, for our purposes we assume the SAMW as one homogenous water mass flowing above the density surface of 26.9 kg/m³. On the transition to the north, the oxygen concentrations rapidly decrease from >4.6 ml/l (CTD 05; Fig. 3e5e) to <1.9 ml/l (CTD 01, 03; Fig. 3f5f) because of respiration and the absence of effective ventilation in the northern Indian Ocean. The reduced vertical changes in salinity north of ~15°S mark the “Indian Equatorial Water” (IEW; Fig. 46). This is described by Sharma (1976), Warren (1981), Quadfasel and Schott (1982), You and Tomczak (1993) and Schott and McCreary (2001) as a mixture of thermocline water masses from the northern and southern Indian Ocean.

4.1.2 Intermediate water masses (26.9–27.34 kg/m³; 800–1000 m)

The salinity minimum (<34.6 PSU) south of 15° S, in a density range of 26.9–27.4 kg/m³ (core density $\sigma=27.2$ kg/m³; Fig. 3a5a) is associated with the “Antarctic Intermediate Water” (AAIW; Fig.4; Bindoff and McDougall, 2000; Deacon, 1933; Fine, 1993; Schott and McCreary, 2001; Toole and Warren, 1993; Warren, 1981; Wyrcki, 1973; You, 1998). It is transported eastwards by the “Antarctic Circumpolar Current” (ACC), penetrates into all three oceans and extends towards the equator to feed the intermediate waters (Fine, 1993; McCartney, 1977; Piola and Gordon, 1989; Reid, 1986, 1989; Sverdrup et al., 1942; Talley, 1996; Wüst, 1935).

The salinity minimum (<34.6 PSU) observed at station CTD 05 (15.08° S; Fig. 3b5b) has a slightly divergent core density (27.0 kg/m³) compared to the AAIW (Fig. 3a5a). This implies a further source to the salinity minimum of the AAIW. A low salinity water mass (~34.8 PSU) flows along 10–15° S (Schott and McCreary, 2001; Wyrcki, 1971; You and Tomczak, 1993) and originates from the ITF. At intermediate depths it has been called “Indonesian Intermediate Water” (IIW; Fig. 46) by Emery and Meincke (1986) and Emery (2001).

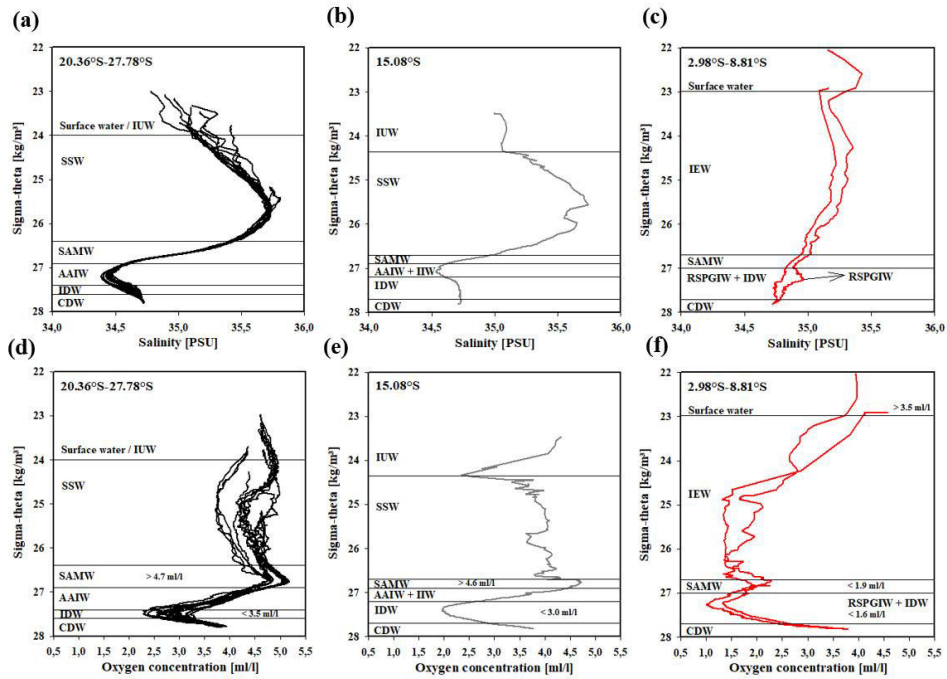
The increase in salinity (>34.9 PSU; Fig. 3e5c) further north, at the same density level as the AAIW, is caused by the inflow of saline water from the Arabian Sea, mainly from the Red Sea outflow (Warren, 1981) and is additionally feedfed by the outflow of the Persian Gulf (Emery and Meincke, 1986). Therefore, this water mass is called “Red Sea-Persian Gulf

Formatiert: Abstand Nach: 12 Pt.

Intermediate Water” (RSPGIW; Fig. 46). The RSPGIW is transported towards the equator and beyond to as far south as 10° S (You, 1998), recirculates in the tropical gyre, and creates the absolute oxygen minimum (<1.1 ml/l) caused by ~~biological~~biogeochemical processes in the Arabian Sea (see Sect. 4.2.1).

5 4.1.3 Deep water masses (>27.34 kg/m³; >1000 m)

Overall, low oxygen concentrations in the northern study area underneath the AAIW (>27.4 kg/m³; Fig. 345f) are caused by in situ consumption (Wyrski, 1962) and reduced ventilation in the northern Indian Ocean. The deep oxygen minimum extends towards the south (~3.0 ml/l) and is associated with the water mass of the “Indian Deep Water” (IDW). The IDW has higher salinities than the overlying AAIW (Bindoff and McDougall, 2000; Mantyla and Reid, 1995; Schott and McCreary, 2001; Talley, 2013) with values of >34.6 PSU below the density range of the AAIW (Fig. 3a5a). The IDW (σ_t ~27.5 kg/m³) flows in the density range just above the “Circumpolar Deep Water” (CDW; Fig. 46) and a further increase in ~~the~~ salinity (34.62–34.73 PSU) and ~~a decrease of~~in the oxygen minimum concentration at the 2°C temperature level (Emery, 2001) ~~marks~~mark the transition between the IDW and the underlying CDW.



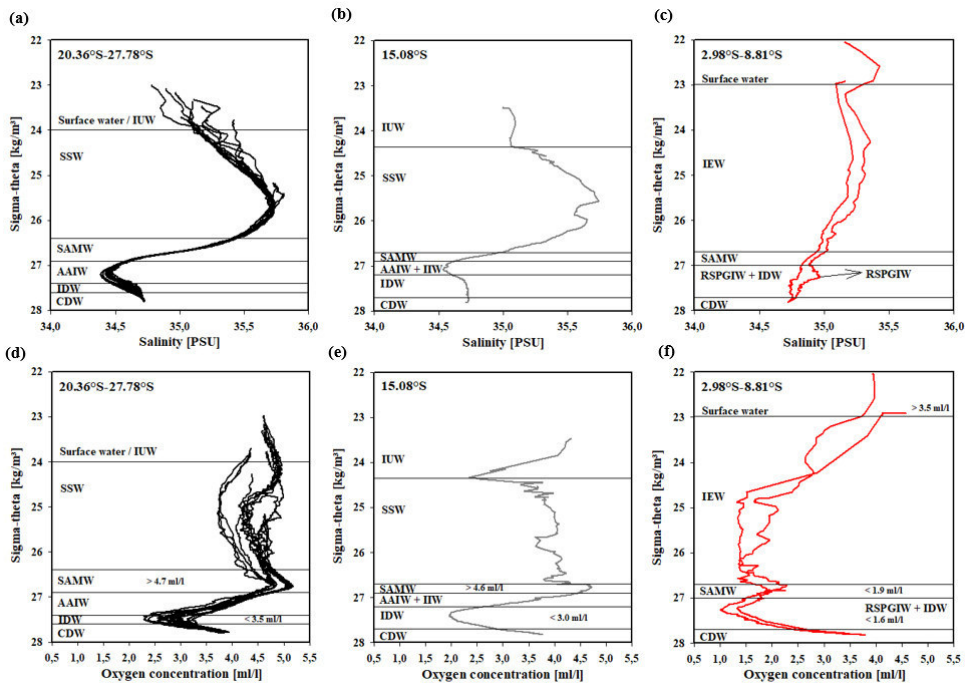


Figure 5: Water mass properties represented as salinity vs. sigma-theta diagrams (a, b, c) and as oxygen vs. sigma-theta diagrams (d, e, f) for CTD stations at latitudes 20.36° S–27.78° S, 15.08° S and 2.98° S–8.81° S. [For water mass abbreviations see Table 1.](#)

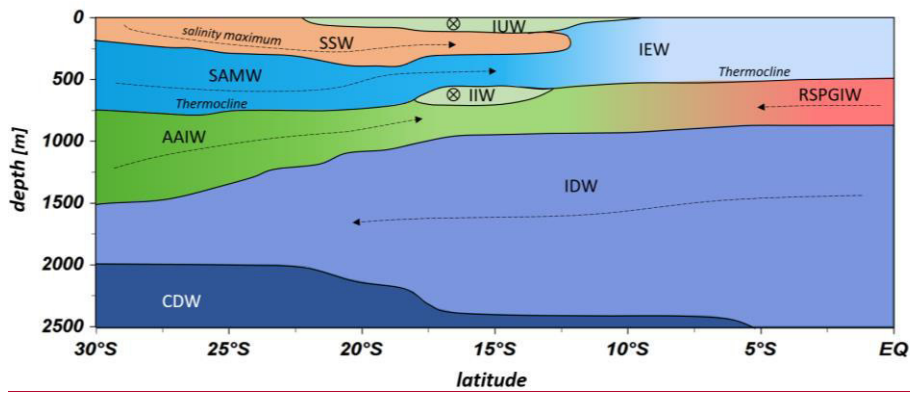
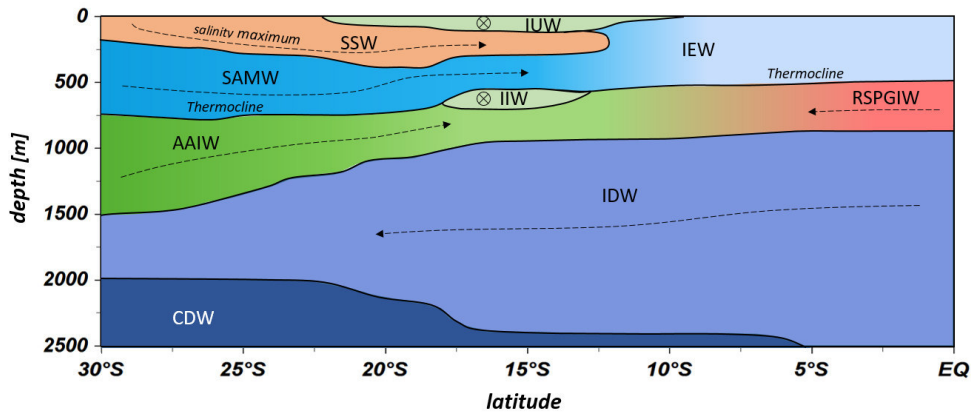


Figure 6: Water mass distribution model from 30° S to the equator. The CTD stations taken into account for this transect ranged between 67.07 °E and 77.16 °E. Indonesian Upper Water (IUW), Subtropical Surface Water (SSW), Subantarctic Mode Water (SAMW), Indian Equatorial Water (IEW), Antarctic Intermediate Water (AAIW), Indonesian Intermediate Water (IIW), Red Sea-Persian Gulf Intermediate Water (RSPGIW), Indian Deep Water (IDW), and Circumpolar Deep Water (CDW). Dotted lines represent N-S current directions and circled crosses indicate latitudinal directions from E to W. For water mass abbreviations see Table 1.

Formatiert: Schriftart: 9 Pt., Nicht Fett

4.2 Nutrient distribution and N-cycle processes in the nitrogen cycle

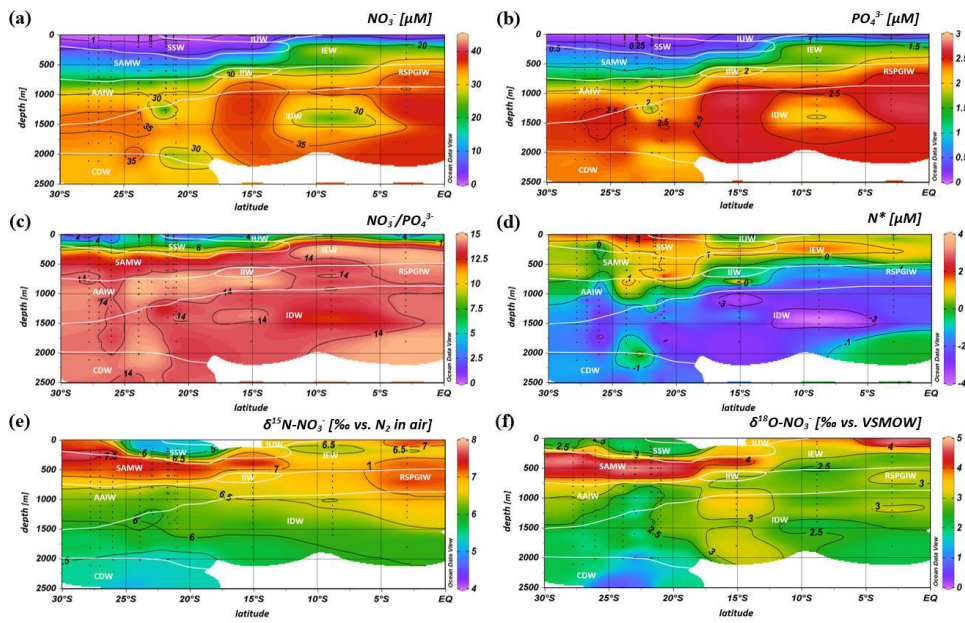
4.2.1 Nutrient supply in the oligotrophic subtropical gyre and lateral transfer across the gyre boundaries

Intense downwelling in the centre of the IOSG is induced by the convergence of horizontal Ekman volume flux (Williams and Follows, 2003) and creates the thick layer of nutrient depleted surface waters within the IUW and SSW (Fig. ~~5a, 5b~~7a, 7b, Table 1), and also within the underlying SAMW. The northward increase in nutrients at $\sim 15^\circ$ S (CTD 05, 2017) marks the northern boundary of the subtropical gyre and the maximum extension of the IUW, SSW, and SAMW. (Table 1). Further increase in nutrient concentrations within the IEW indicate the transition from the subtropical gyre towards the southern equatorial Indian Ocean ~~indicated~~identified by the characteristic shoaling of the nutricline at the northern fringe of the gyre.

(Table 1, Fig. 7a, 7b). The IEW is not a well-defined water mass, but rather a mixture of thermocline waters from the South Indian Ocean and from the nutrient-enriched northern Indian Ocean. Therefore, just below the upper 100 m nutrient concentrations increase ~~towards~~up to $\sim 23 \mu\text{M}$ nitrate and $\sim 1.6 \mu\text{M}$ phosphate (Table 1) at the northernmost stations (CTD 01, 03; 2017) and indicate ~~more and more~~the increasing influence of the nutrient-enriched northern Indian Ocean (Gaye et al., 2013). This increased northern influence is also reflected by the $\text{NO}_3/\text{PO}_4^{3-}$ ratios, which ~~indicates~~exhibit values of less than 8 in the upper 200 m of the subtropical gyre ~~and, but~~ increase towards the southern equatorial Indian Ocean, tracking the outcropping nutriclines (Fig. 5e7c). Low $\text{NO}_3/\text{PO}_4^{3-}$ ratios are typical in surface waters of oligotrophic regions because nitrate commonly becomes depleted ~~before~~prior to phosphate (Gruber and Sarmiento and Gruber, 2006; Deutsch et al., 2007).

Due to the intense downwelling in the centre of the IOSG, the supply of nutrients by vertical mixing is reduced or absent in the gyre (Williams and Follows, 1998). ~~Therefore~~Thus, lateral transfer across the gyre boundaries and biologically induced in -situ processes (e.g., N_2 -Fixation) are ~~the~~ major processes supplying nutrients to the euphotic zone of the subtropical gyre.

Formatiert: Abstand Vor: 18 Pt.



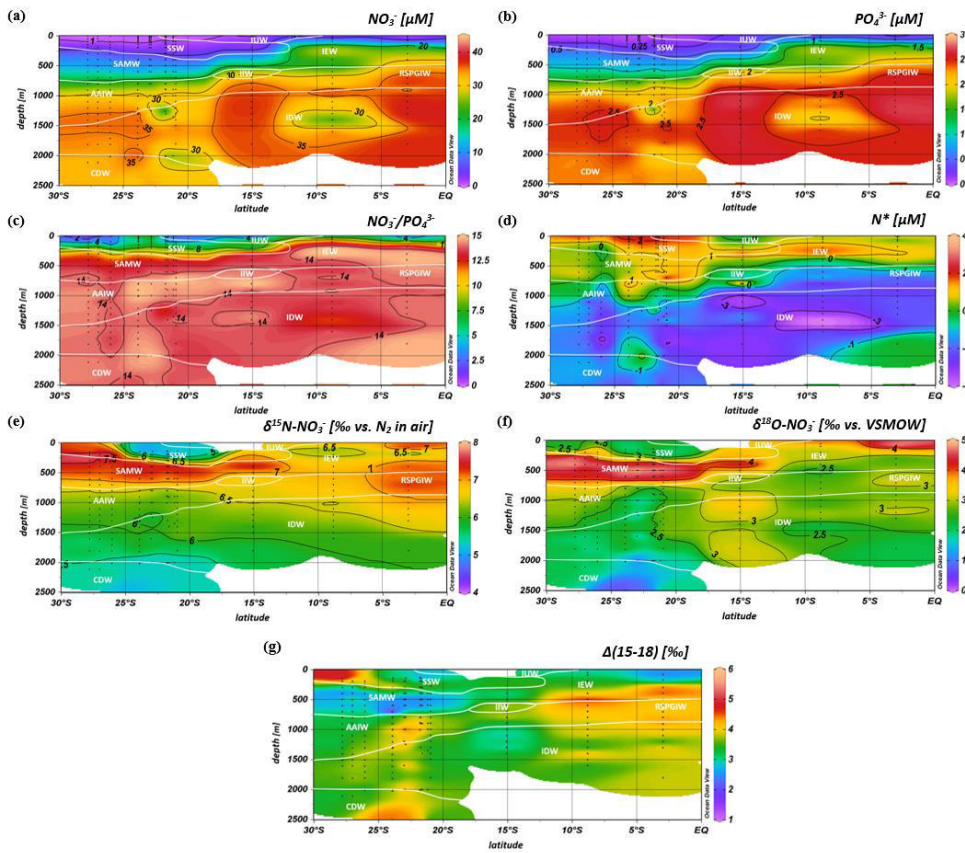


Figure 7: Profiles: Latitudinal profiles from south to north with an overlay of the water mass distribution [model](#) (white contour lines) in the South Indian Ocean of nitrate (a) and phosphate concentrations (b), $\text{NO}_3^-/\text{PO}_4^{3-}$ ratio (c), N^* (d), and $\delta^{15}\text{N}$ of nitrate- NO_3^- (e) and $\delta^{18}\text{O}$ - NO_3^- of nitrate (f-) and nitrate $\Delta(15-18)$ as the difference between $\delta^{15}\text{N}\text{-NO}_3^-$ and $\delta^{18}\text{O}\text{-NO}_3^-$. For water mass abbreviations see [Fig. 6](#).

5

Formatiert: Schriftart: 9 Pt., Englisch (Vereinigte Staaten)

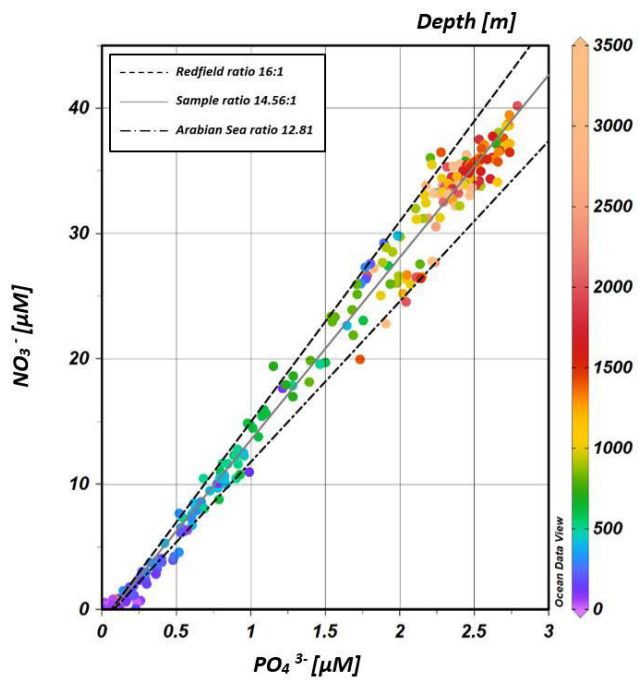
The water masses entering the study area from the [south Southern Ocean](#) and from the [southern equatorial/northern](#) Indian Ocean have characteristic nutrient concentrations and isotope fingerprints of reactive nitrogen, so that some of the water masses are clearly discernible by the distribution of nutrients and the isotopic composition of nitrate within the IOSG. Our samples

show $\text{NO}_3/\text{PO}_4^{3-}$ ratios of 14.56 on average (Fig. 68). These ~~results differ from $\text{NO}_3/\text{PO}_4^{3-}$ ratios are lower than~~ the global ocean mean of 16:1 (Redfield, 1934, 1963) ~~and reveal a lower $\text{NO}_3/\text{PO}_4^{3-}$ ratio.~~ Furthermore, measurements in the Arabian Sea reveal typical $\text{NO}_3/\text{PO}_4^{3-}$ ratios of ~ 12.81 (Codispoti et al., 2001), even lower than our detected $\text{NO}_3/\text{PO}_4^{3-}$ ratios. Consequently, the average $\text{NO}_3/\text{PO}_4^{3-}$ ratio of 14.56 falls between the global ocean mean of 16:1 (Redfield, 1934, 1963) and the typical ratio in the Arabian Sea of ~ 12.81 (Codispoti et al., 2001). This alone indicates the mixing of water masses of southern and northern Indian Ocean origin.

The deviation from the Redfield stoichiometry (Bourbonnais et al., 2009; Redfield, 1934, 1963) is quantified by the tracer N^* (~~Eq. the analytical error of our N^* estimate based on the relative error of nitrate and phosphate analyses, which was below 1–5 % for duplicate sample measurements~~). The Arabian Sea is characterised by an extensive oxygen deficit zone (ODZ) that induces denitrification in mid-water depths (150–400 m) (Gaye et al., 2013) and leads to an N deficit ~~in the water column and therefore to negative N^* values~~ (e.g., Bange et al., 2005; Rixen et al., 2005; Gaye et al., 2013). ~~A deficit of N is expressed by a negative N^* that in our Our~~ data set ~~has reveals~~ values of about $-1 \mu\text{M}$ within the RSPGIW and values lower than $-4 \mu\text{M}$ within the IDW (Fig. 5d, 7d), ~~which coincide with the oxygen minimum (see Sect. 4.1). Consequently, negative N^* values are a result of the influx of water masses from the Arabian Sea, which are characterised by denitrification. To strengthen this assumption and to compensate the limitations of the N^* approach mentioned before, we use stable isotope measurements.~~

~~These negative N^* values are imported to intermediate and deep waters within the subtropical gyre and coincide with the oxygen minimum (see Sect. 4.1). Consequently, negative N^* values are a result of the influx of water masses from the Arabian Sea.~~

Formatiert: Englisch (Vereinigtes Königreich)



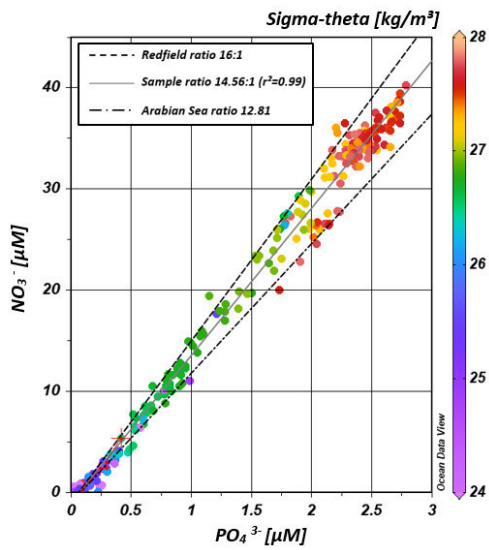


Figure 8: Correlation of nitrate versus phosphate concentrations. Regression line of the sample pool (solid, grey line) indicates a ratio of ~14.56, ($r^2=0.99$), intermediate between the Redfield ratio of 16:1 (black, dashes line) and the mean ratio in the Arabian Sea with a slope of ~12.81 (grey, dotted-dashed line) after Codispoti et al. (2001). Color-coding of dots indicates the potential density σ_t in kg/m^3 .

The denitrification signal, transported by the RSPGIW and IDW into the IOSG, is also detected in isotope signatures. Denitrification discriminates against the heavier isotope of nitrate (^{15}N , ^{18}O), and raises $\delta^{15}\text{N}$ and $\delta^{18}\text{O}$ in equal proportions. Our measurements indicate we observe elevated $\delta^{15}\text{N}$ and $\delta^{18}\text{O}$ values of $>7\%$ and $>3\%$ within the RSPGIW at CTD 01 and 03 (Fig. 5e, 5f; Table 1, Figs. 7e, 7f) accompanied by nitrate concentrations of $>30\ \mu\text{M}$ (Fig. 5a, 7a). Denitrification discriminates against the heavier isotope of nitrate (^{15}N , ^{18}O) and raises $\delta^{15}\text{N}$ as well as $\delta^{18}\text{O}$. In the Arabian Sea average $\delta^{15}\text{N}$ and $\delta^{18}\text{O}$ values of $>20\%$ and $>15\%$, respectively, are observed in mid-water depth (150–400 m) (Gaye et al., 2013). The significant progressive reduction of $\delta^{15}\text{N}$ and $\delta^{18}\text{O}$ towards the south to the IOSG South Indian Ocean is a result of mixing with other subtropical thermocline water masses contributing to the IEW and of respiration of relatively more ^{15}N -depleted organic matter remineralisation/N-assimilation processes along the flow path.

Within the IOSG, $\delta^{15}\text{N}$ and $\delta^{18}\text{O}$ are also elevated within the SAMW (400–500 m) with values of $>7\%$ and $>4\%$ (Fig. 5e, 5f). However, compared with the Within the RSPGIW and the lower IEW, we observe a deviation

from the O-to-N isotope effect of $\epsilon^{18\text{O}}:\epsilon^{15\text{N}} \sim 1$ that is typical for consumption processes like denitrification (Granger et al., 2004; Rafter et al., 2013; Sigman et al., 2003; Sigman et al., 2005). The difference between N and O isotopes ($\delta^{15\text{N}} - \delta^{18\text{O}}$) can be quantified by the tracer $\Delta(15-18)$ that indicates values of $>4\text{‰}$ within the RSPGIW and the lower IEW (Figure 7g). The RSPGIW injects nitrate that is remineralised from $^{15\text{N}}$ -enriched organic matter, originated in a region of strong denitrification.

5 During remineralisation of organic matter, the N isotope effect associated with ammonium production and nitrification does not affect the $\delta^{15\text{N}}\text{-NO}_3^-$ but depends on the biomass being remineralised (Rafter et al., 2013). In contrast, the $\delta^{18\text{O}}$ of newly nitrified nitrate is independent of the isotopic composition of the organic matter and leads to a counteracting behaviour of $\delta^{15\text{N}}$ and $\delta^{18\text{O}}$. Therefore, the RSPGIW adds nitrate that is enhanced in $\delta^{15\text{N}}$ compared to the ambient water and drives the decoupling of N and O isotopes. Furthermore, the source nitrate for N-assimilation in the lower IEW is this regenerated nitrate
10 and results also in the decoupling of N and O isotopes in this depth range. Consequently, the elevated $\Delta(15-18)$ can be explained by a remineralisation/N-assimilation cycle and by the lateral influx of $^{15\text{N}}$ -enriched nitrate induced by strong denitrification in the Arabian Sea.

In the IOSG, we observe elevated $\delta^{15\text{N}}$ and $\delta^{18\text{O}}$ values of $>7\text{‰}$ and $>4\text{‰}$ (Table 1, Figs. 7e, 7f) within the SAMW (400–500 m) that is originated in the Subantarctic thermocline of the Southern Ocean. RSPGIW, this pool has distinctly lower
15 nitrate concentrations of $<20\text{ }\mu\text{M}$, which indicates another formation mechanism. The mechanism that elevated the isotope ratios in the SAMW is due to surface processes in the Subantarctic, where this water mass originates. In general, N-assimilation has an isotopic effect of about 5–10‰ (Montoya and McCarthy, 1995; Sigman et al., 2005; Waser et al., 1998) and produces biomass that is relatively depleted in $^{15\text{N}}$ and $^{18\text{O}}$ in comparison to the nitrate source. Consequently, this drives the elevation in $\delta^{15\text{N}}$ and $\delta^{18\text{O}}$ of the remaining nitrate as uptake proceeds. In However, in oligotrophic waters, such as in the IOSG, this
20 isotopic effect is not expressed/observable (Montoya et al., 2002); as nitrate is typically drawn down to the limit of detection by complete N-assimilation. Therefore, the elevated isotope values in the SAMW are a transport signal from the Subantarctic region and not a result of in situ processes in the gyre.

Nitrate in surface waters of the Southern Ocean is only partially assimilated due to light limitation and less iron availability (DiFiore/Boyd et al., 2000; DiFiore et al., 2006; DiFiore et al., 2010; Hutchins et al., 2001; Sigman et al., 1999) and when this
25 surface water is subducted, its nitrate pool has typical leads to $\delta^{15\text{N}}$ values of $\sim 5\text{--}9\text{‰}$ (up to $\sim 13\text{‰}$) (DiFiore et al., 2006; Sigman et al., 1999, 2000). This. Seasonal mixing and remineralisation processes result in $\delta^{15\text{N}}$ values of 5–9‰ within Subantarctic thermocline waters (McCartney, 1977; Sigman et al., 1999). On its flow path towards the north, this isotope trace of incomplete assimilation causes the elevated isotope values within the SAMW that enters the subtropical Indian Ocean thermocline with $\delta^{15\text{N}}$ values of $>7\text{‰}$ from the Southern Ocean (Table 3; Figs. 5e, 7a; Table 1, Figs. 4c, 7e, 9a).

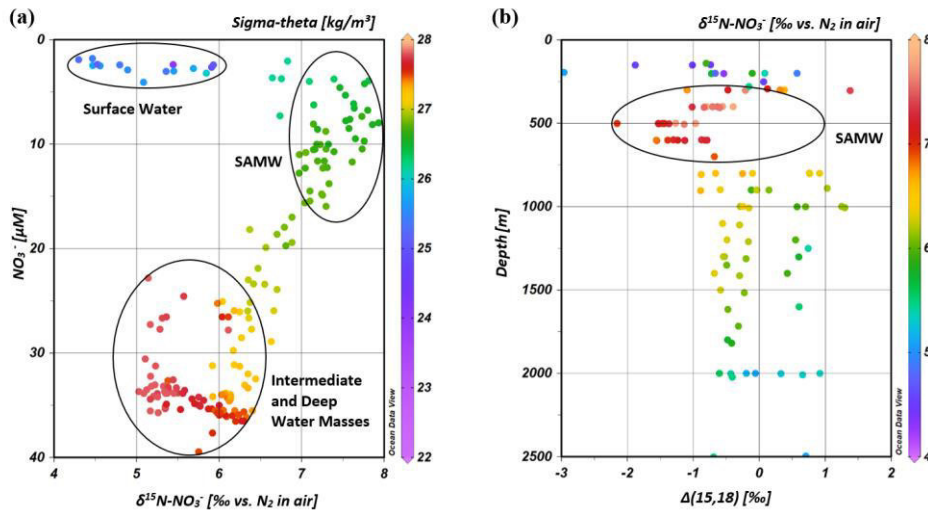


Figure 7: Nitrate concentrations versus $\delta^{15}\text{N}$ of nitrate for CTD stations within the IOSG (a). Color code of dots indicates the potential density sigma-theta (kg/m^3). Figure 7b represents the tracer $\Delta(15,18)$ versus water depth, where colored dots represent Subantarctic thermocline waters, the $\delta^{15}\text{N}$ of nitrate for CTD stations between 17°S source water of the SAMW and 25°S .

5

The underlying AAIW in the IOSG, we compare the nitrate isotope properties match measurements in the Southern Ocean south of 40°S by of Subantarctic thermocline waters with our results. Sigman et al. (1999, 2000) and DiFiore et al. (2006). They use the correlation of $\delta^{15}\text{N}$ and the fraction of nitrate remaining - $\ln(\text{NO}_3^-)$ - to quantify the isotope fractionation effect during N-uptakeassimilation in the Antarctic and Subantarctic region. If N-uptakeassimilation occurs with a constant effect and no new nitrate is added to the surface ocean, then the uptake process can be described in terms of Rayleigh fractionation kinetics (Mariotti et al., 1981). To fulfil the conditions of Rayleigh fractionation, the nitrate samples plot along a straight line in $\delta^{15}\text{N}/\ln(\text{NO}_3^-)$ space, where the slope of the line represents the isotope effect of N-uptake or mixing of different nitrate pools. Sigman et al. (1999, 2000) and DiFiore et al. (2006) compare the theoretically Rayleigh utilization trend within the Subantarctic thermocline, where Sigman et al., (1999, 2000) determined a slope of $\delta^{15}\text{N}/\ln(\text{NO}_3^-) \sim 1.3 \text{‰}$ (Fig. 8).

15

Subantarctic thermocline waters are the source water of the SAMW and the underlying AAIW in the IOSG (9b). Our results reveal a similar nitrate utilization signal with a slightly, but even shallower regression lineslope of $\delta^{15}\text{N}/\ln(\text{NO}_3^-) \sim 0.93 \text{‰}$ (Fig.

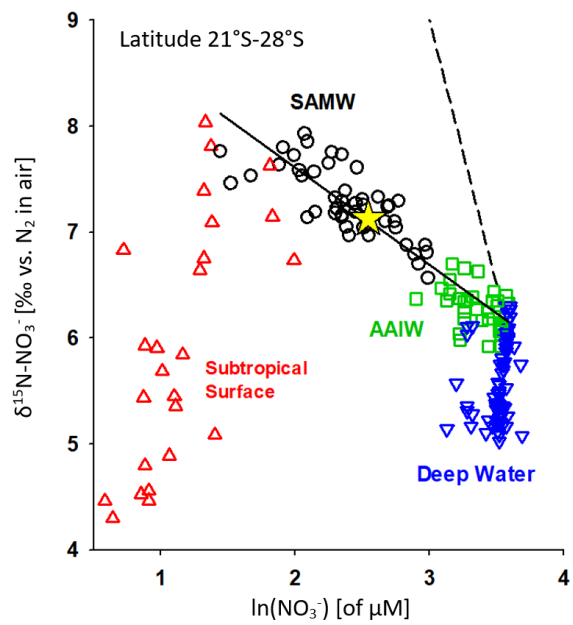
Formatiert: Schriftart: 10 Pt.

Formatiert: Schriftart: 10 Pt.

Formatiert: Schriftart: Calibri

Formatiert: Schriftart: Calibri

~~89b~~). It is clearly a mixing signal that causes the moderate slopes of $\delta^{15}\text{N}/\ln(\text{NO}_3)$ in both the gyre region and in the Subantarctic because biological utilisation of nitrate is unlikely ~~-~~ at this depth range. The explanation for the slightly shallower slope in our data set compared to the results in the Subantarctic is vertical mixing with the overlying SSW that has lower $\delta^{15}\text{N}$ values (<6 ‰) with nitrate concentrations of <5 μM ~~and a~~ This process does not fulfil conditions of Rayleigh fractionation because
5 of fundamentally different formation background (Table 1, Fig. 7a9a; see Sect. 4.2.2). Deep-water nitrate concentrations vary little and $\delta^{15}\text{N}$ increases towards ~~lower~~ shallower water depths and the nitrate ~~utilisation~~ signal slightly differ from that of the Southern Ocean due to the influence of the IDW , originated in the Northern Indian Ocean.



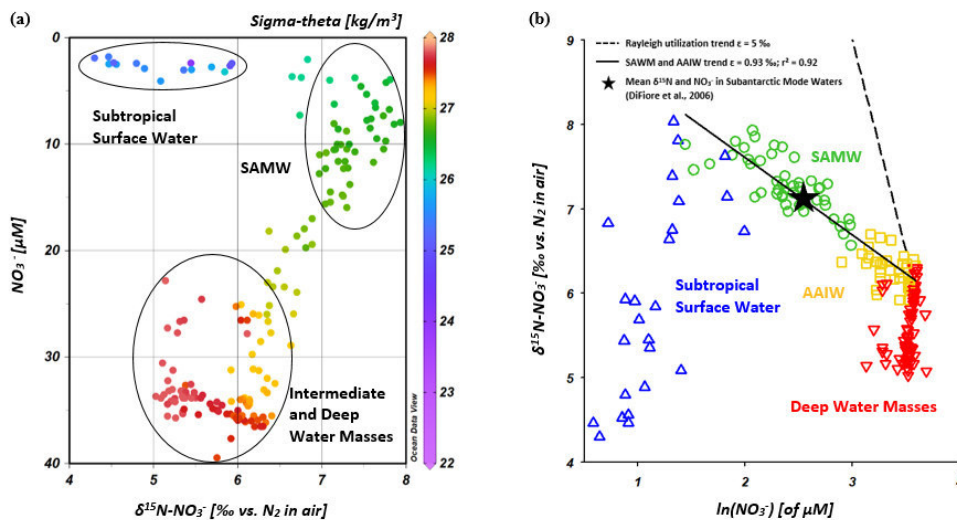


Figure 9: The $\delta^{15}\text{N}$ of nitrate, Nitrate concentrations versus $\delta^{15}\text{N}\text{-NO}_3^-$ (a) and $\delta^{15}\text{N}\text{-NO}_3^-$ versus $\ln(\text{NO}_3^-)$ (b) for CTD stations at latitude 21°S – 28°S . Data were within the IOSG (20.36°S – 27.78°S). Colour-code of dots in Fig. 9a indicates the potential density sigma-theta (kg/m^3). In Fig. 9b, data is grouped for the subtropical surface water (blue), SAMW (green), AAIW (yellow) and deep water. The regression line of samples within the masses (red SAMW and AAIW (solid line) is similar to that in the Subantarctic thermocline (Sigman et al., 1999, 2000). The dashed line illustrates the Rayleigh nitrate utilization trend with a slope of 5%. The yellow star marks the mean $\delta^{15}\text{N}$ of nitrate (7.1‰) and NO_3^- (12.8 μM) of SAMW in the Subantarctic region after DiFiore et al. (2006).

Within the isotope maxima of the **SAMW** (~500 m), the uniform evolution of N and O isotopes of nitrate breaks down; accompanied by and reveals an offset (of about 100 m) of between the depths of the N and O isotopic maxima at 23.91°S – 20.36°S (Table 3) (Figs. 4c, 4d and see supplement tables S2 and S3). Both, $\delta^{15}\text{N}$ and $\delta^{18}\text{O}$, are elevated within the SAMW, but $\delta^{15}\text{N}$ is less elevated than $\delta^{18}\text{O}$. The decoupling of N and O isotopes is expressed by the tracer $\Delta(15,18)$ (see Eq. 2) that is sensitive with regard to source signatures. Therefore, we adopt the CDW as the source water and source nitrate pool ($\delta^{15}\text{N}_{\text{deep}}=5.5\text{‰}$; $\delta^{18}\text{O}_{\text{deep}}=1.7\text{‰}$) for the subtropical region. Consequently, less elevation of $\delta^{15}\text{N}$ compared to $\delta^{18}\text{O}$ leads to a negative $\Delta(15,18)$.

Negative $\Delta(15,18)$ values of $\leq -0.5 < 3\text{‰}$ (Fig. 7b) arise within the SAMW and may be an indirect effect of the partial N-assimilation, that is originated in the partially assimilated Subantarctic region. Isotope fractionation during the initial phase of partial N-assimilation leads to sinking organic matter that is more depleted in ^{15}N than the source nitrate (Sigman et

- Formatiert: Schriftart: 9 Pt., Fett
- Formatiert: Schriftart: 9 Pt.
- Formatiert: Standard, Abstand Vor: 6 Pt., Zeilenabstand: einfach
- Formatiert: Schriftart: 9 Pt.
- Formatiert: Schriftart: 9 Pt.
- Formatiert: Schriftart: 9 Pt.
- Formatiert: Schriftart: 9 Pt.
- Formatiert: Schriftart: 9 Pt.
- Formatiert: Schriftart: 9 Pt.

Formatiert: Englisch (Vereinigte Staaten)

al., 1999; Rafter et al., 2013). ~~Remineralization~~ While the influx of this sinking the SAWM into the subtropical gyre injects ~~^{15}N depleted~~ organic matter, ~~organic matter remineralisation~~ adds nitrate that is depleted in ^{15}N and lowers the $\delta^{15}\text{N}$ of the ambient nitrate and thus leads to a ~~negative~~ low $\Delta(15-18)$ ~~from the N isotope side in subtropical thermocline waters (Fig. 7g)~~. To conclude, ~~remineralization~~ ~~remineralisation~~ of organic matter produced by partial N-assimilation in the Southern Ocean ~~indicates a negative~~ is reflected in lower $\Delta(15-18)$ and leads to the deviation of the isotope maxima with an offset of 100 m within the depth range of the SAMW. However, the ~~remineralization~~ ~~remineralisation~~ of ^{15}N -depleted organic matter formed out of newly fixed ~~N~~ nitrogen from N_2 -fixation in surface waters may also ~~drives~~ influence the decrease of $\Delta(15-18)$ (see the following Sect. 4.2.2).

4.2.2 Evidence for N_2 -fixation in the SIOG IOSG

The mixing of source water signals from the lateral influx of the neighbouring northern Indian Ocean and Southern Ocean ~~are important influences on~~ significantly affects the nutrient distribution and isotopic composition of nitrate in the gyre region. However, N^* and $\delta^{15}\text{N}$ also suggest that N_2 -fixation is an important process within the IOSG and introduces new nitrate into the surface waters of the IOSG. The increase in N^* increased up to $1.5-2 \mu\text{M}$ at 60–200 m and is an evidence for the input of newly fixed N that shifts m indicates a positive deviation of the $\text{NO}_3/\text{PO}_4^{3-}$ ratio from the Redfield stoichiometry to higher ratios (Bourbonnais et al., 2009; Gruber and Sarmiento, 1997; Redfield, 1934, 1963). Such shifts also have been attributed to and is an evidence for the input of newly fixed N into the surface water. Studies in the South-West Pacific Ocean also indicate positive N^* anomalies of $\sim 2 \mu\text{M}$ in the productive layer reflecting diazotrophic N_2 -fixation (Fumenia et al., 2018). Although N_2 -fixation is the first order driver of positive N^* (Bourbonnais et al., 2009; Monteiro and Follows, 2006), other processes, for instance atmospheric deposition or the preferential ~~remineralization~~ ~~remineralisation~~ of N over P and results, may also be responsible for excess N and result in an overestimation of N^* . However, a first order driver of positive N^* clearly is ~~is~~-based N_2 -fixation (Bourbonnais et al., 2009; Monteiro and Follows, 2006).

~~We~~ However, the South Indian Ocean is less affected by the influx of nutrient enriches mineral aerosols from atmospheric deposition (Duce et al., 2008; Duce and Tindale, 1991) and we neglect this fact in our further discussion. Furthermore, we use $\delta^{15}\text{N}$ and $\delta^{18}\text{O}$ of nitrate, as well as $\Delta(15-18)$, as additional indicators of N sources to overcome the weakness associated with the N^* approach.

Diazotrophic N_2 -fixation produces organic matter that has a low $\delta^{15}\text{N}$ relative to average oceanic combined nitrogen (Carpenter et al., 1997; Minagawa and Wada, 1986; Montoya et al., 2002; Wada and Hattori, 1976). Within the surface waters (<250 upper 200 m) of the IOSG ($\sim 17(20.36^\circ \text{S} - 25(23.91^\circ \text{S})$), the $\delta^{15}\text{N}$ of nitrate is lower than varies between 4.3‰ and 5.9‰ with a mean of $\sim 5.0 \text{‰}$ (Figs. 5e, 7a). Although this δ value is high (e. 9a, 9b). These values are higher compared to other regions of intense N_2 -fixation, such as in the oligotrophic Northsubtropical NE Atlantic, where values near -1 to -2‰ are common (Montoya et al., 2002), contradict the assumption of N_2 -fixation of $2-5 \text{‰}$ occur in surface waters within the IOSG (Bourbonnais et al., 2009). At first sight, the high values of surface waters in the IOSG do not speak for significant N_2 -fixation in surface waters.

Formatiert: Tiefgestellt

However, considering ~~that SAMW and SSW as~~ the ~~sources for injection~~ source of nutrients into the gyre nitrate with elevated $\delta^{15}\text{N}$ values of >7.0 (-174 ‰ on average (20.36°S – 2523.91°S)) and highest values of 7.9 ‰ (Figs. 9a, 9b, see also supplement table S2), the $\delta^{15}\text{N}$ is clearly reduced in surface waters (4.3 – 5.9 ‰) is lowered by ~ 2.4 ‰. This indicates an addition of is similar to the decrease of ~ 3 ‰ in surface waters of the north Atlantic, where N_2 -fixation is verified (Bourbonnais et al., 2009; Knapp et al., 2008). Therefore, N_2 -fixation is most likely the main driver in the upward decrease of $\delta^{15}\text{N}$ in surface waters and adds isotopically light N nitrogen from the atmosphere into the gyre region from 17°S to 25°S (Fig. 7a).

Furthermore, To prove this, we take the nitrate $\delta^{18}\text{O}$ into account, which exhibits values of <3 ‰ and shows a minor decrease compared to $\delta^{15}\text{N}$. This The resulting decoupling of N and O isotopes of nitrate again leads to a negative $\Delta(15,18)$, a typical indicator of N_2 -fixation. Several lines of evidence thus show that N_2 -fixation occurs in the subtropical gyre: the negative $\Delta(15,18)$ of <-0.5 ‰ down to 250 m (Fig. 7b), accompanied by distinctly low $\delta^{15}\text{N}$ (Fig. 5c), and elevated N^* of >1 μM (Fig. 5d). These smaller differences between $\delta^{15}\text{N}$ and $\delta^{18}\text{O}$ and reveals a $\Delta(15-18)$ of <3 ‰ (Fig. 7g). To conclude, positive N^* values, distinct upward decrease of $\delta^{15}\text{N}$ - NO_3^- , reduced $\Delta(15-18)$ and the distance from any external nitrate sources are unambiguous evidences of diazotrophic activity within the surface layer.

To estimate the supply of newly fixed N to the nutrient pool, we calculate the fraction of nitrate coming from N_2 -fixation with the following equation:

$$\text{NO}_3^-/\text{PO}_4^{3-} \text{ cat} = \text{NO}_3^- \text{ sample} / \left(\frac{\text{NO}_3^- \text{ in}}{\text{NO}_3^-/\text{PO}_4^{3-} \text{ in}} - \frac{\text{NO}_3^- \text{ ass}}{\text{NO}_3^-/\text{PO}_4^{3-} \text{ ass}} \right) \quad (51)$$

with “ $\text{NO}_3^- \text{ in}$ ” as initial nitrate concentration of the source water (SAMW within the IOSG and IEW in the southern equatorial region), “ $\text{NO}_3^- \text{ ass}$ ” denoting the assimilated nitrate ($\text{NO}_3^- \text{ in} - \text{NO}_3^- \text{ sample}$) and “ $\text{NO}_3^- \text{ sample}$ ” being the sample concentrations. The initial nitrate to phosphate pool $\text{NO}_3^-/\text{PO}_4^{3-} \text{ in}$ is defined as mean ratio of the source water. For the region of the IOSG, we presume that the mean ratio within the SAMW is 13.25 and 14.25 in the southern equatorial Indian Ocean. For N-assimilation in the euphotic zone we assume Redfield conditions of $\text{NO}_3^-/\text{PO}_4^{3-} \text{ ass} = 16$. To calculate the residual nitrate, we multiply the calculated nitrate to phosphate ratio ($\text{NO}_3^-/\text{PO}_4^{3-} \text{ cat}$) with the measured phosphate concentrations:

$$\text{NO}_3^- \text{ cat} = \frac{\text{NO}_3^-/\text{PO}_4^{3-} \text{ cat}}{\text{PO}_4^{3-} \text{ sample}} \quad (6\text{NO}_3^-/\text{PO}_4^{3-} \text{ sample}) \quad (2)$$

The difference of $\text{NO}_3^- \text{ sample}$ and $\text{NO}_3^- \text{ cat}$ represents the portion of the nitrate formed/supplied by nitrification out of newly fixed N, which is consumed by N-assimilation under Redfield conditions. At latitude 1720.36°S – 2523.91°S , our samples indicate elevated $\text{NO}_3^-/\text{PO}_4^{3-}$ ratios and a resulting positive deviation from the calculated line of N-assimilation at nitrate concentrations of <10 μM (Fig. 9a10a). Consequently, N_2 -fixation leads to the local elevation in $\text{NO}_3^-/\text{PO}_4^{3-}$ ratios due to the input of new N and coincide with the decrease of $\delta^{15}\text{N}$ and the decoupling of N and O isotopes, leading to a negative/low $\Delta(15-18)$. The quantity of newly fixed nitrate ($\text{NO}_3^- \text{ fixew}$) is given by the formula

Formatiert: Englisch (Vereinigtes Königreich)

$$NO_3^-_{fix} / NO_3^-_{new} [in \%] = \frac{(NO_3^-_{sample} - NO_3^-_{cal})}{NO_3^-_{sample}} * 100 \quad , \quad (73)$$

which is ~~represented~~ presented in Fig. 9b10b, indicating a distinct upward increase in the upper 200 m at 1720.36° S–2523.91° S with an average portion of fixed nitrate of about 34 %, suggesting %.

5 ~~suggests~~ that about one-third of the nitrate measured in the upper 200 m is derived from newly fixed nitrogen. ~~To prove this, we can calculate the $\delta^{15}N$ that has to be adjusted in surface waters when we assume that 34 % of the assimilated nitrate is provided from newly fixed nitrogen.~~ Considering a $\delta^{15}N$ of 0 ‰ for atmospheric N_2 and an average $\delta^{15}N$ of 7.34 ‰ of the source water (SAMW) ~~and a $\delta^{15}N$ of 0 ‰ for the atmospheric N_2 ,~~ we can calculate a $\delta^{15}N-NO_3^-_{fix/new}$ of ~4.8 ‰ ~~in the surface water. 9 ‰.~~ Our measurements show an average $\delta^{15}N-NO_3^-$ of ~5.40 ‰ in the upper 200 m with a minimum of 4.3 ‰ (CTD 10 52; 2016) and a maximum of 5.9 ‰ (CTD 32; 2016) and hence, agree ~~with the calculated $\delta^{15}N-NO_3^-$ quite well with the calculated $\delta^{15}N-NO_3^-_{new}$.~~ Bourbonnais et al. (2009) stated that N_2 -fixation accounts for ~40 % of newly supplied nitrate in the subtropical North Atlantic. This is slightly higher than our assumption for the subtropical South Indian Ocean. However, in the subtropical North Atlantic higher N^* values (3.5 μM), a slightly stronger upward decrease of $\delta^{15}N$ and a stronger decoupling of N and O isotopes are observed in surface waters, suggesting higher fixation rates.

Formatiert: Englisch (Vereinigtes Königreich)

Formatiert: Englisch (Vereinigtes Königreich)

Formatiert: Englisch (Vereinigtes Königreich)

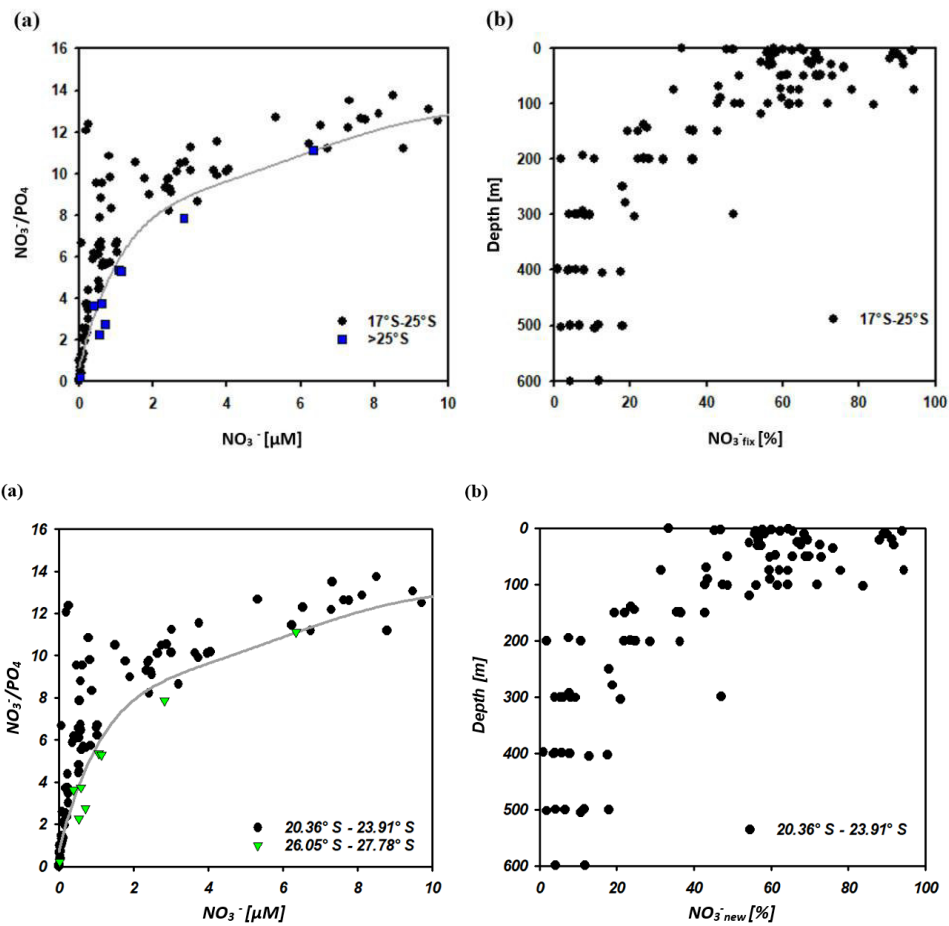


Figure 10: $\text{NO}_3^-/\text{PO}_4^{3-}$ ratio versus nitrate concentrations of seawater samples at $17.20.36^\circ\text{S}$ – $25.23.91^\circ\text{S}$ and $>25.26.05$ – 27.78°S (a). The grey solid line indicates the calculated N-assimilation ($\text{NO}_3^-_{\text{cal}}$ vs. $\text{NO}_3^-/\text{PO}_4^{3-}_{\text{cal}}$) with a preformed $\text{NO}_3^-:\text{PO}_4^{3-}$ in ratio of 13.25 for the region of the IOSG and 14.25 for the southern equatorial Indian Ocean and progressive nutrient assimilation with a Redfield ratio of 16 ($\text{NO}_3^-/\text{PO}_4^{3-}$ ass). In Fig. 9b10b we present the portion of nitrate formed out of newly fixed N ($\text{NO}_3^-_{\text{new}}$) versus depth at latitudes $17.20.36^\circ\text{S}$ – $25.23.91^\circ\text{S}$.

Formatiert: Schriftart: Fett

Further south (≈ 25 at 26.05 – 27.78° S), samples plot close to the line of N-assimilation and no significant input of fixed nitrate is indicated (Fig. 9a10a). This agrees with the $\delta^{15}\text{N}$ values in surface waters, indicating the same which demonstrate an abrupt increase at about 26° S to similar values as in the underlying SAMW ($>7\%$), while $\delta^{18}\text{O}$ shows still low values of $<3\%$. Consequently, N and O isotopes show/reveal a counteracting behaviour that differs from the region at $\approx 20.36^\circ$ S– 25.91° S, resulting in a positive high $\Delta(15-18)$ of $>0.5\%$ (Fig. 5g7g). This is evidence a strong indication for the absence of N_2 -fixation in this region but also indicates leads to the assumption that $\delta^{18}\text{O}$ remains low due to ongoing nitrate production by nitrification.

Formatiert: Englisch (Vereinigtes Königreich)

This sudden termination of N_2 -fixation in the tropical may be due to a temperature-limiting factor, mentioned by Capone et al. (1997) and Breitbarth et al. (2007). They argue that N_2 -fixation by *Trichodesmium*, which is the dominant nitrogen-fixing cyanobacteria in subtropical oceans is restricted to areas with oligotrophic waters (Berman-Frank et al., 2001; Pearl et al., 1994), decreases dramatically at seawater temperatures in the range of 20 – 30°C below 22°C (Capone/Berman-Frank et al., 1997; Breitbarth et al., 2007/2001). Modelling N_2 -fixation with this assumption thus resulted in very limited/low fixation rates south of about 25° S, although phosphate and iron are not limiting in the Indian Ocean (Paulsen et al., 2017). At latitudes north of 25° S, where we see a significant contribution of N_2 -fixation, surface temperatures exceed 20°C , and reach up to 29°C (S1). In comparison, south of 25° S, where however, N_2 -fixation is not detectable, we observe sea surface temperatures of 20.5°C on average, and less by other diazotrophs (e.g., unicellular diazotrophic cyanobacteria) has been shown to occur at higher latitudes than 20°C just below *Trichodesmium* (Moisander et al., 2010). Another reason for the surface. These lower temperatures can thus explain the absence/decline of N_2 -fixation south of 25° S.

Formatiert: Englisch (Vereinigte Staaten)

Conclusions

The subtropical gyre 26° S may be limited availability of iron and other micronutrients. Atmospheric iron deposition is low in the southern hemisphere oceans and iron availability gradually decreases towards high southern latitudes (Boyd et al., 2000; Duce and Tindale, 1991; Duce et al., 2008). Reduced iron availability is suggested to limit growth of nitrogen-fixing organisms in regions of already limited iron availability (Sanudo-Wilhelmy et al., 2001). Berman-Frank et al. (2001) calculated the potential of nitrogen fixation by *Trichodesmium* and suggested that in 75% of the global ocean, iron availability limits nitrogen fixation. However, until now no concrete studies on iron and other micronutrient availability and N_2 -fixation have been conducted within the South Indian Ocean is one of five gyres in the world's oceans, which develop extensive oligotrophic regions.

Formatiert: Schriftfarbe: Schwarz, Englisch (Vereinigtes Königreich), Unterschneidung ab 16 Pt.

Formatiert: Schriftfarbe: Schwarz, Englisch (Vereinigtes Königreich), Unterschneidung ab 16 Pt.

Conclusion

The South Indian Ocean gyre (IOSG) is the only oligotrophic gyre in the Indian Ocean due to the land-locked nature of the northern Indian Ocean. Compared to the Atlantic and Pacific Ocean gyres the IOSG is less explored and is poorly understood in terms of nutrient distribution and isotopic composition of nitrate.

- 5 This work compiles the general distribution of water masses from 30° S, within the IOSG, across the South Equatorial Current (SEC), and towards the southern equatorial Indian Ocean. ~~The~~ We established the first water mass distribution model in this ocean region that provides a basis for the identification of nutrient sources and the isotopic signatures of nitrate, ~~which are among the first reported in this region~~. Water masses in our study area are diverse and originate in two fundamentally different ocean regimes: ~~In~~ the Southern Ocean (SAMW and AAIW) and ~~in~~ the northern Indian Ocean (RSPGIW and IDW). These different water masses have a major influence on the nutrient distribution and stable isotope composition of nitrate in the IOSG.

- 10 ~~The patterns~~ Our nutrient and isotopic data, which are the first reported for the subtropical South Indian Ocean, demonstrate the lateral influx from the Arabian Sea, characterized by strong denitrification in mid-water depths that leads to an N deficit in intermediate and deep waters accompanied by elevated isotope ratios of nitrate within the RSPGIW. The lateral influx from the Southern Ocean is via the oxygen saturated SAMW, with characteristically elevated isotope ratios of nitrate due to partial N-assimilation in ~~the~~ high southern latitudes.

- 15 Additionally, ~~the~~ our data mirror an external input of N by N₂-fixation that is indicated by positive N* and ~~negative~~ low $\Delta(15\text{-}18)$ values in surface waters. In the upper 200 m ~~of~~ in the region ~~of~~ 20.36° S–23.91° S, we calculate that approximately ~~one third~~ 34 % of the nitrate consumed by N-assimilation is provided ~~by~~ from newly fixed nitrogen.

- 20 The IOSG has been sparsely investigated and is an area representing those oceanic oligotrophic regions that are likely to adjust to continued warming by deepening stratification, reduced upward nutrient supply across the thermocline, and decreasing biological production. Whether this will be offset by enhanced N₂-fixation in warming surface ~~is~~ layers remains as an open question that needs dedicated follow-up studies, ~~both~~ *i.e.*, in terms of experimental approaches, time series observation, remote sensing, and biogeochemical modelling.

Formatiert: Englisch (Vereinigtes Königreich)

Formatiert: Englisch (Vereinigtes Königreich)

Formatiert: Englisch (Vereinigtes Königreich)

Formatiert: Schriftart: +Textkörper (Times New Roman), 12 Pt., Kursiv, Schriftfarbe: Text 1, Englisch (Vereinigte Staaten)

~~*Data availability.* The data will be available in the data publisher PANGAEA.~~

Data availability. All data of cruises SO 259 and MSM 59/2 are available at the PANGAEA data publisher for Earth & Environmental Science. The data can be found under Harms, Natalie; Lahajnar, Niko; Gaye, Birgit; Rixen, Tim; Dähnke, Kirstin; Ankele, Markus; Schwarz-Schampera, Ulrich; Emeis, Kay-Christian (2019): Physical oceanography, nutrients, and nitrogen and oxygen isotopic composition of nitrate measured on water bottle samples during Maria S. Merian cruise MSM59/2. PANGAEA, <https://doi.pangaea.de/10.1594/PANGAEA.897503> and Harms, Natalie; Lahajnar, Niko; Gaye, Birgit; Rixen, Tim; Dähnke, Kirstin; Ankele, Markus; Schwarz-Schampera, Ulrich; Emeis, Kay-Christian (2019): Physical oceanography, nutrients, and nitrogen and oxygen isotopic composition of nitrate measured on water bottle samples during SONNE cruise SO259. PANGAEA, <https://doi.pangaea.de/10.1594/PANGAEA.897504>.

10 *Author contribution.* N. Lahajnar and N. C. Harms collected the samples on board. U. Schwarz-Schampera conceived the INDEX program in the IOSG and ~~lead~~led the cruises. N. Lahajnar, B. Gaye, T. Rixen and K.-C. Emeis designed the nutrient and nitrogen cycle study. N. C. Harms, N. Lahajnar, K. Dähnke and M. Ankele participated in the sample analyses. N. C. Harms, N. ~~Lahjnar~~Lahajnar and B. Gaye analysed the data. N. C. Harms wrote the first draft of the manuscript. All authors contributed substantially to the final paper

15 *Competing interests.* The authors declare that they have no conflict of interest.

Acknowledgments. Cruises and sampling were conducted ~~in~~within the framework of the INDEX program of the Federal Institute for Geosciences and Natural Resources (BGR). The INDEX program explores polymetallic sulfides on the ocean floor, based on a fifteen-year contract of BGR with the International Seabed Authority. BGR requests acknowledgment in any future use of the data and results in this publication. We thank the crew of the ~~German~~ research vessels *Maria S. Merian* and

20 *Sonne* for ~~supporting~~their outstanding support of our work on board. Furthermore, we thank our colleagues, from the Helmholtz Institute *Geesthacht*, especially Tina Sanders, ~~in~~Geesthacht for supporting our analyses of nutrients and stable isotopes of nitrate.

References

- Bange, H. W., Naqvi, S. W. A., and Codispoti, L.: The nitrogen cycle in the Arabian Sea. *Prog. Oceanogr.*, 65(2-4), 145-158, <https://doi.org/10.1016/j.pocan.2005.03.002>, 2005.
- Baumgartner, A., and Reichel, E.: The world water balance: Mean annual global, continental and maritime precipitation evaporation and run-off: Elsevier Science Inc, 1975.
- Behrenfeld, M. J., O'Malley, R. T., Siegel, D. A., McClain, C. R., Sarmiento, J. L., Feldman, G. C., Milligan, A. J., Falkowski, P. G., Letelier, R. M., and Boss, E. S.: Climate-driven trends in contemporary ocean productivity. *Nature*, 444(7120), 752, 2006.
- Berman-Frank, I., Cullen, J. T., Shaked, Y., Sherrell, R. M. and Falkowski, P. G.: Iron availability, cellular iron quotas, and nitrogen fixation in *Trichodesmium*. *Limnol. Oceanogr.*, 46(6), 1249-1260. <https://doi.org/10.4319/lo.2001.46.6.1249>, 2001.
- Bianchi, M., Feliatra, F., Tréguer, P., Vincendeau, M.-A., and Morvan, J.: Nitrification rates, ammonium and nitrate distribution in upper layers of the water column and in sediments of the Indian sector of the Southern Ocean. *Deep-sea Res. Pt. II*, 44(5), 1017-1032, [https://doi.org/10.1016/S0967-0645\(96\)00109-9](https://doi.org/10.1016/S0967-0645(96)00109-9), 1997.
- Bindoff, N. L., and McDougall, T. J.: Decadal changes along an Indian Ocean section at 32°S and their interpretation. *J. Phys. Oceanogr.*, 30(6), 1207-1222, [https://doi.org/10.1175/1520-0485\(2000\)030<1207:DCAAIO>2.0.CO;2](https://doi.org/10.1175/1520-0485(2000)030<1207:DCAAIO>2.0.CO;2), 2000.
- Böhlke, J. K., Mroczkowski, S. J., and Coplen, T. B.: Oxygen isotopes in nitrate: new reference materials for 18O:17O:16O measurements and observations on nitrate-water equilibration. *Rapid Commun. Mass Sp.*, 17(16), 1835-1846, <https://doi.org/10.1002/rcm.1123>, 2003.
- Bourbonnais, A., Lehmann, M. F., Wanek, J. J., and Schulz-Bull, D. E.: Nitrate isotope anomalies reflect N₂ fixation in the Azores Front region (subtropical NE Atlantic). *J. Geophys. Res.-Oceans*, 114(C3), n/a-n/a, <https://doi.org/10.1029/2007JC004617>, 2009.
- Boyd, P. W., Watson, A. J., Law, C. S., Abraham, E. R., Trull, T., Murdoch, R., Bakker, D. C. E., Bowie, A. R., Buesseler, K. O., Chang, H., Charette, M., Croot, P., Downing, K., Frew, R., Gall, M., Hadfield, M., Hall, J., Harvey, M., Jameson, G., LaRoche, J., Liddicoat, M., Ling, R., Maldonado, M. T., McKay, R. M., Nodder, S., Pickmere, S., Pridmore, R., Rintoul, S., Safi, K., Sutton, P., Strzepek, R., Tanneberger, K., Turner, S., Waite, A., and Zeldis, J.: A mesoscale phytoplankton bloom in the polar Southern Ocean stimulated by iron fertilization. *Nature*, 407, 695. <https://doi.org/10.1038/35037500>, 2000.

Formatiert: Englisch (Vereinigtes Königreich)

Formatiert: Englisch (Vereinigtes Königreich)

- Brandes, J. A., Devol, A. H., Yoshinari, T., Jayakumar, D. A., and Naqvi, S. W. A.: Isotopic composition of nitrate in the central Arabian Sea and eastern tropical North Pacific: A tracer for mixing and nitrogen cycles. *Limnol. Oceanogr.*, 43(7), 1680-1689, <https://doi.org/10.4319/lo.1998.43.7.1680>, 1998.
- Breitbarth, E., Oschlies, A., and LaRoche, J.: Physiological constraints on the global distribution of *Trichodesmium* - effect of temperature on diazotrophy. *Biogeosciences*, 4(1), 53-61, 2007.
- Capone, D. G., Zehr, J. P., Paerl, H. W., Bergman, B., and Carpenter, E. J.: *Trichodesmium*, a Globally Significant Marine Cyanobacterium. *Science*, 276(5316), 1221-1229, <https://doi.org/10.1126/science.276.5316.1221>, 1997.
- Carpenter, E. J., Harvey, H. R., Fry, B., and Capone, D. G.: Biogeochemical tracers of the marine cyanobacterium *Trichodesmium*. *Deep-Sea Res. Pt. I*, 44(1), 27-38, [https://doi.org/10.1016/S0967-0637\(96\)00091-X](https://doi.org/10.1016/S0967-0637(96)00091-X), 1997.
- 10 Casciotti, K. L., Sigman, D. M., Hastings, M. G., Böhlke, J., and Hilkert, A.: Measurement of the oxygen isotopic composition of nitrate in seawater and freshwater using the denitrifier method. *Anal. Chem.*, 74(19), 4905-4912, <https://doi.org/10.1021/ac020113w>, 2002.
- Casciotti, K. L., Trull, T., Glover, D., and Davies, D.: Constraints on nitrogen cycling at the subtropical North Pacific Station ALOHA from isotopic measurements of nitrate and particulate nitrogen. *Deep Sea Research Part II: Topical Studies in Oceanography*, 55(14-15), 1661-1672. <https://doi.org/10.1016/j.dsr2.2008.04.017>, 2008.
- 15 Clark, D. R., Rees, A. P., and Joint, I.: Ammonium regeneration and nitrification rates in the oligotrophic Atlantic Ocean: Implications for new production estimates. *Limnol. Oceanogr.*, 53(1), 52-62. <https://doi.org/10.4319/lo.2008.53.1.0052>, 2008.
- Codispoti, L., Brandes, J. A., Christensen, J., Devol, A., Naqvi, S., Paerl, H. W., and Yoshinari, T.: The oceanic fixed nitrogen and nitrous oxide budgets: Moving targets as we enter the anthropocene? *Sci. Mar.*, 65(S2), 85-105, 2001.
- 20 Colborn, J. G.: *The thermal structure of the Indian Ocean*. University Press of Hawaii Honolulu, 1975.
- Deacon, G. E.: A general account of the hydrology of the South Atlantic Ocean. *Discovery Reports*, 7, 171-238, 1933.
- Deutsch, C., Gruber, N., Key, R. M., and L., S. J.: Denitrification and N₂ fixation in the Pacific Ocean. *Global Biogeochem. Cy.*, 15(2), 483-506, <https://doi.org/10.1029/2000GB001291>, 2001.
- 25 Deutsch, C., Sarmiento, J. L., Sigman, D. M., Gruber, N., and Dunne, J. P.: Spatial coupling of nitrogen inputs and losses in the ocean. *Nature*, 445, 163, <https://doi.org/10.1038/nature05392>, 2007.
- DiFiore, P. J., Sigman, D. M., Trull, T. W., Lourey, M. J., Karsh, K., Cane, G., and Ho, R.: Nitrogen isotope constraints on subantarctic biogeochemistry. *J. Geophys. Res.-Oceans*, 111(C8), n/a-n/a, <https://doi.org/10.1029/2005JC003216>, 2006.

Formatiert: Englisch (Vereinigtes Königreich)

DiFiore, P. J., Sigman D. M., Karsh Kristen, L., Trull Thomas, W., Dunbar Robert, B., and Robinson Rebecca, S. (2010). Poleward decrease in the isotope effect of nitrate assimilation across the Southern Ocean. *Geophys. Res. Lett.*, 37(17), <https://doi.org/10.1029/2010GL044090>, 2010.

5 [Duce, R. A., and Tindale, N. W.: Atmospheric transport of iron and its deposition in the ocean. *Limnology and Oceanography*, 36\(8\), 1715-1726, <https://doi.org/10.4319/lo.1991.36.8.1715>, 1991.](#)

[Duce, R., LaRoche, J., Altieri, K., Arrigo, K., Baker, A., Capone, D., Cornell, S., Dentener, F., Galloway, J., and Ganeshram, R.: Impacts of atmospheric anthropogenic nitrogen on the open ocean. *Science*, 320\(5878\), 893-897. <https://doi.org/10.1126/science.1150369>, 2008.](#)

Duing, W.: The monsoon regime of the currents in the Indian Ocean: Hawaii inst of Geophysics Honolulu, 1970.

10 Emerson, S., Mecking, S., and Abell, J.: The biological pump in the subtropical North Pacific Ocean: Nutrient sources, Redfield ratios, and recent changes. *Global Biogeochem. Cy.*, 15(3), 535-554, <https://doi.org/10.1029/2000GB001320>, 2001.

Emery, W. J.: Water types and water masses. *Encyclopedia of ocean sciences*, 6, 3179-3187, <https://doi.org/10.1006/rwos.2001.0108>, 2001.

Emery, W. J., and Meincke, J.: Global water masses: summary and review. *Oceanologica Acta*, 9, 383-391, 1986.

15 Fine, R. A.: Circulation of Antarctic intermediate water in the South Indian Ocean. *Deep-Sea Res.h Pt. I*, 40(10), 2021-2042, [https://doi.org/10.1016/0967-0637\(93\)90043-3](https://doi.org/10.1016/0967-0637(93)90043-3), 1993.

[Fumenia, A., Moutin, T., Bonnet, S., Benavides, M., Petrenko, A., Helias Nunige, S., and Maes, C.: Excess nitrogen as a marker of intense dinitrogen fixation in the Western Tropical South Pacific Ocean: impact on the thermocline waters of the South Pacific, *Biogeosciences Discuss. Biogeosciences Discuss.*, 10, 2018.](#)

20 Gaye, B., Nagel, B., Dähnke, K., Rixen, T., and Emeis, K. C. (2013). Evidence of parallel denitrification and nitrite oxidation in the ODZ of the Arabian Sea from paired stable isotopes of nitrate and nitrite. *Global Biogeochem. Cy.*, 27(4), 1059-1071, <https://doi.org/10.1002/2011GB004115>, 2013.

25 Gaye-Haake, B., Lahajnar, N., Emeis, K.-C., Unger, D., Rixen, T., Suthhof, A., Ramaswamy, V., Schulz, H., Paropkari, A., and Guptha, M.: Stable nitrogen isotopic ratios of sinking particles and sediments from the northern Indian Ocean. *Mar. Chem.*, 96(3-4), 243-255, <https://doi.org/10.1016/j.marchem.2005.02.001>, 2005.

~~Godfrey, J., and Golding, T.: The Sverdrup relation in the Indian Ocean, and the effect of Pacific-Indian Ocean throughflow on Indian Ocean circulation and on the East Australian Current. *J. Phys. Oceanogr.*, 11(6), 771-779, [https://doi.org/10.1175/1520-0485\(1981\)011<0771:TSRITI>2.0.CO;2](https://doi.org/10.1175/1520-0485(1981)011<0771:TSRITI>2.0.CO;2), 1981.~~

Formatiert: Englisch (Vereinigtes Königreich)

Granger, J., Sigman D. M., Needoba Joseph, A., and Harrison Paul, J.: Coupled nitrogen and oxygen isotope fractionation of nitrate during assimilation by cultures of marine phytoplankton. *Limnol. Oceanogr.*, 49(5), 1763-1773, <https://doi.org/10.4319/lo.2004.49.5.1763>, 2004.

Grasshoff, K., Kremling, K., and Ehrhardt, M.: *Methods of seawater analysis*: John Wiley and Sons, 2009.

- 5 Gruber, N., and Sarmiento, J. L.: Global patterns of marine nitrogen fixation and denitrification. *Global Biogeochem. Cy.*, 11(2), 235-266, <https://doi.org/10.1029/97GB00077>, 1997.

~~Gruber, N., and Sarmiento, J. L., Herraiz-Borreguero, L., and Rintoul, S. R.: Subantarctic mode water: distribution and circulation. *Ocean Dynamics*, 61(1), 103-126, <https://doi.org/10.1007/s10236-010-0352-9>, 2011.~~

- 10 ~~Hutchins, D., Sedwick, P., DiTullio, G., Boyd, P., Queguiner, B., Griffiths, F., and Crossley, C.: Control of phytoplankton growth by iron and silicic acid availability in the subantarctic Southern Ocean: Experimental results from the SAZ Project. *Journal of Geophysical Research: Oceans*, 106(C12), 31559-31572, <https://doi.org/10.1029/2000JC000333>, 2001.~~

~~*Ocean biogeochemical dynamics*: Princeton University Press, 2006.~~

Karl, D. M., Letelier, R., Hebel, D., Tupas, L., Dore, J., Christian, J., and Winn, C.: Ecosystem changes in the North Pacific subtropical gyre attributed to the 1991–92 El Niño. *Nature*, 373, 230, <https://doi.org/10.1038/373230a0>, 1995.

- 15 ~~Knapp, A. N., DiFiore, P. J., Deutsch, C., Sigman, D. M., and Lipschultz, F.: Nitrate isotopic composition between Bermuda and Puerto Rico: Implications for N₂ fixation in the Atlantic Ocean. *Global Biogeochemical Cycles*, 22(3), <https://doi:10.1029/2007GB003107>, 2008.~~

20 Lehmann, M. F., Sigman, D. M., McCorkle, D. C., Brunelle, B. G., Hoffmann, S., Kienast, M., Cane, G., and Clement, J.: Origin of the deep Bering Sea nitrate deficit: Constraints from the nitrogen and oxygen isotopic composition of water column nitrate and benthic nitrate fluxes. *Global Biogeochem. Cy.*, 19(4), <https://doi.org/10.1029/2005GB002508>, 2005.

Mantyla, A. W., and Reid, J. L.: On the origins of deep and bottom waters of the Indian Ocean. *J. Geophys. Res.-Oceans*, 100(C2), 2417-2439, <https://doi.org/10.1029/94JC02564>, 1995.

- 25 Mariotti, A., Germon, J., Hubert, P., Kaiser, P., Letolle, R., Tardieux, A., and Tardieux, P.: Experimental determination of nitrogen kinetic isotope fractionation: some principles; illustration for the denitrification and nitrification processes. *Plant soil*, 62(3), 413-430, <https://doi.org/10.1007/BF02374138>, 1981.

McCartney, M. S.: *Subantarctic Mode Water, A Voyage of Discovery, George Deacon 70th Anniversary Volume* M. Angel, 103–119: Pergamon, New York, 1977.

McCartney, M. S.: The subtropical recirculation of mode waters. *J. Mar. Res.*, 40(436), 427-464, 1982.

Formatiert: Links, Einzug: Links: 0 cm, Hängend: 1,27 cm, Abstand Nach: 12 Pt., Zeilenabstand: Mehrere 1,15 ze

Formatiert: Abstand Nach: 12 Pt.

- McClain, C. R., Signorini, S. R., and Christian, J. R.: Subtropical gyre variability observed by ocean-color satellites. *Deep-Sea Res. Pt. II*, 51(1), 281-301, <https://doi.org/10.1016/j.dsr2.2003.08.002>, 2004.
- Michaels, A., Olson, D., Sarmiento, J., Ammerman, J., Fanning, K., Jahnke, R., Knap, A., Lipschultz, F., and Prospero, J.: Inputs, losses and transformations of nitrogen and phosphorus in the pelagic North Atlantic Ocean. *Biogeochemistry*, 35(1), 181-226, <https://doi.org/10.1007/BF02179827>, 1996.
- Minagawa, M., and Wada, E.: Nitrogen isotope ratios of red tide organisms in the East China Sea: A characterization of biological nitrogen fixation. *Mar. Chem.*, 19(3), 245-259, [https://doi.org/10.1016/0304-4203\(86\)90026-5](https://doi.org/10.1016/0304-4203(86)90026-5), 1986.
- Moisander, P. H., Beinart, R. A., Hewson, I., White, A. E., Johnson, K. S., Carlson, C. A., Montoya, J. P., and Zehr, J. P.: Unicellular cyanobacterial distributions broaden the oceanic N₂ fixation domain. *Science*, 327(5972), 1512-1514, <https://doi.org/10.1126/science.1185468>, 2010.
- Monteiro, F. M., and Follows, M.: Nitrogen fixation and preferential remineralization of phosphorus in the North Atlantic: Model insights. *Eos, Transactions, American Geophysical Union*, 87(36), 2006.
- Montoya, J. P., and McCarthy, J. J.: Isotopic fractionation during nitrate uptake by phytoplankton grown in continuous culture. *J. Plankton Res.*, 17(3), 439-464, <https://doi.org/10.1093/plankt/17.3.439>, 1995.
- Montoya, J. P., Carpenter, E. J., and Capone, D. G.: Nitrogen fixation and nitrogen isotope abundances in zooplankton of the oligotrophic North Atlantic. *Limnol. Oceanogr.*, 47(6), 1617-1628, <https://doi.org/10.4319/lo.2002.47.6.1617>, 2002.
- ~~Montoya, J. P., and McCarthy, J. J.: Isotopic fractionation during nitrate uptake by phytoplankton grown in continuous culture. *J. Plankton Res.*, 17(3), 439-464, <https://doi.org/10.1093/plankt/17.3.439>, 1995.~~
- Murontsev, A.: Osnovnye cherty gidrologii Indijskogo okeana (The Main Features of Indian Ocean Hydrology). *Gidrometeoizdat, Leningrad*, 1959.
- Murphy, J., and Riley, J. P.: A modified single solution method for the determination of phosphate in natural waters. *Anal. Chim. acta*, 27, 31-36, [https://doi.org/10.1016/S0003-2670\(00\)88444-5](https://doi.org/10.1016/S0003-2670(00)88444-5), 1962.
- Paerl, H. W., Prufert-Bebout, L. E., and Guo, C.: Iron-stimulated N₂ fixation and growth in natural and cultured populations of the planktonic marine cyanobacteria *Trichodesmium* spp. *Appl. Environ. Microbiol.*, 60(3), 1044-1047, 1994.
- Paulsen, H., Ilyina, T., Six, K. D., and Stemmler, I.: Incorporating a prognostic representation of marine nitrogen fixers into the global ocean biogeochemical model HAMOCC. *J. Adv. Model. Earth Sy.*, 9(1), 438-464, <https://doi.org/10.1002/2016MS000737>, 2017.
- Pickard, G., and Emery, W.: *Descriptive physical Oceanography*, 249 pp. Pergamon, Tanytown, NY, 1982.

- Piola, A. R., and Gordon, A. L.: Intermediate waters in the southwest South Atlantic. *Deep-Sea Res.*, 36(1), 1-16, [https://doi.org/10.1016/0198-0149\(89\)90015-0](https://doi.org/10.1016/0198-0149(89)90015-0), 1989.
- Quadfasel, D. R., and Schott, F.: Water-mass distributions at intermediate layers off the Somali Coast during the onset of the southwest monsoon, 1979. *J. Phys. Oceanogr.*, 12(12), 1358-1372, [https://doi.org/10.1175/1520-0485\(1982\)012<1358:WMDAIL>2.0.CO;2](https://doi.org/10.1175/1520-0485(1982)012<1358:WMDAIL>2.0.CO;2), 1982.
- Rafter, P. A., DiFiore, P. J., and Sigman, D. M.: Coupled nitrate nitrogen and oxygen isotopes and organic matter remineralization in the Southern and Pacific Oceans. *J. Geophys. Res.-Oceans*, 118(10), 4781-4794, <https://doi.org/10.1002/jgrc.20316>, 2013.
- Redfield, A. C.: On the proportions of organic derivatives in sea water and their relation to the composition of plankton. *James Johnstone memorial volume*, 176-192, 1934.
- Redfield, A. C.: The influence of organisms on the composition of seawater. *The sea*, 2, 26-77, 1963.
- Reid, J. L.: On the total geostrophic circulation of the South Pacific Ocean: Flow patterns, tracers and transports. *Prog. Oceanogr.*, 16(1), 1-61, [https://doi.org/10.1016/S0079-6611\(97\)00012-8](https://doi.org/10.1016/S0079-6611(97)00012-8), 1986.
- Reid, J. L.: On the total geostrophic circulation of the South Atlantic Ocean: Flow patterns, tracers, and transports. *Prog. Oceanogr.*, 23(3), 149-244, [https://doi.org/10.1016/0079-6611\(89\)90001-3](https://doi.org/10.1016/0079-6611(89)90001-3), 1989.
- Rixen, T., and Ittekkot, V.: Nitrogen deficits in the Arabian Sea, implications from a three component mixing analysis. *Deep-Sea Res. Pt. II*, 52(14-15), 1879-1891, <https://doi.org/10.1016/j.dsr2.2005.06.007>, 2005.
- [Sanudo-Wilhelmy, S. A., Kustka, A. B., Gobler, C. J., Hutchins, D. A., Yang, M., Lwiza, K., Burns, J., Capone, D. G., Raven, J. A. and Carpenter, E. J.: Phosphorus limitation of nitrogen fixation by *Trichodesmium* in the central Atlantic Ocean. *Nature* 411, 66-69. <https://doi.org/10.1038/35075041>, 2001.](#)
- [Sarmiento, J. L., and Gruber, N.: *Ocean biogeochemical dynamics*: Princeton University Press, 2006.](#)
- Schott, F. A., and McCreary, J. P.: The monsoon circulation of the Indian Ocean. *Prog. Oceanogr.*, 51(1), 1-123, [https://doi.org/10.1016/S0079-6611\(01\)00083-0](https://doi.org/10.1016/S0079-6611(01)00083-0), 2001.
- Sharma, G.: Transequatorial movement of water masses in the Indian Ocean. *J. Mar. Res.*, 1976.
- [Sigman, D. M., and Casciotti, K. L.: Nitrogen isotopes in the Ocean. In J. H. Steele, K. K. Turekian and S. A. Thorpe \(Eds.\), *Encyclopedia of ocean sciences* \(pp. 1884-1894\). New York: Elsevier, 2001.](#)
- [Sigman, D. M., Altabet, M. A., McCorkle, D. C., Francois, R., and Fischer, G.: The \$\delta^{15}\text{N}\$ of nitrate in the southern ocean: Consumption of nitrate in surface waters. *Global Biogeochem. Cy.*, 13\(4\), 1149-1166, <https://doi.org/10.1029/1999GB900038>, 1999.](#)

Formatiert: Links, Einzug: Links: 0 cm, Hängend: 1,27 cm, Abstand Nach: 12 Pt., Zeilenabstand: Mehrere 1,15 ze

- Sigman, D. M., Altabet, M. A., McCorkle, D. C., Francois, R., and Fischer, G.: The $\delta^{15}\text{N}$ of nitrate in the Southern Ocean: Nitrogen cycling and circulation in the ocean interior. *J. Geophys. Res.-Oceans*, 105(C8), 19599-19614, <https://doi.org/10.1029/2000JC000265>, 2000.
- Sigman, D. M., and Casciotti, K. L.: Nitrogen isotopes in the Ocean. In J. H. Steele, K. K. Turekian and S. A. Thorpe (Eds.), *Encyclopedia of ocean sciences* (pp. 1884-1894). New York: Elsevier, 2001.
- ~~Sigman, D. M.,~~ Robinson, R., Knapp, A., Van Geen, A., McCorkle, D., Brandes, J., and Thunell, R.: Distinguishing between water column and sedimentary denitrification in the Santa Barbara Basin using the stable isotopes of nitrate. *Geochem. Geophys. Geosy.*, 4(5), <https://doi.org/10.1029/2002GC000384>, 2003.
- Sigman, D. M., Granger, J., DiFiore, P. J., Lehmann, M. M., Ho, R., Cane, G., and van Geen, A.: Coupled nitrogen and oxygen isotope measurements of nitrate along the eastern North Pacific margin. *Global Biogeochem. Cy.*, 19(4), <https://doi.org/10.1029/2005GB002458>, 2005.
- Sigman, D. M., Karsh, K. L., and Casciotti, K. L.: *Ocean process tracers: nitrogen isotopes in the ocean*, Elsevier Ltd, 2009.
- Sverdrup, H. U., Johnson, M. W., and Fleming, R. H.: *The Oceans: Their Physics, Chemistry, and General Biology*. Prentice Hall NY, 1942.
- Talley, L. D.: Antarctic intermediate water in the South Atlantic The South Atlantic (pp. 219-238): Springer, <https://doi.org/10.1029/95JC00858>, 1996.
- Talley, L. D.: Closure of the Global Overturning Circulation Through the Indian, Pacific, and Southern Oceans, *Schematics and Transports. Oceanography*, 26(1), 80-97, 2013.
- Toole, J. M., and Warren, B. A.: A hydrographic section across the subtropical South Indian Ocean. *Deep-Sea Res. Pt. I*, 40(10), 1973-2019, [https://doi.org/10.1016/0967-0637\(93\)90042-2](https://doi.org/10.1016/0967-0637(93)90042-2), 1993.
- Wada, E., and Hattori, A.: Natural abundance of ^{15}N in particulate organic matter in the North Pacific Ocean. *Geochim. Cosmochim. Ac.*, 40(2), 249-251, [https://doi.org/10.1016/0016-7037\(76\)90183-6](https://doi.org/10.1016/0016-7037(76)90183-6), 1976.
- Wankel, S. D., Kendall, C., Pennington, J. T., Chavez, F. P., and Paytan, A.: Nitrification in the euphotic zone as evidenced by nitrate dual isotopic composition: Observations from Monterey Bay, California. *Global Biogeochemical Cycles*, 21(2), <https://doi.org/10.1029/2006GB002723>, 2007.
- Ward, B., Devol, A., Rich, J., Chang, B., Bulow, S., Naik, H., ~~et al~~Pratihary, A., and Jayakumar, A.: Denitrification as the dominant nitrogen loss process in the Arabian Sea. *Nature*, 461(7260), 78, 2009.
- Warren, B. A.: Transindian hydrographic section at Lat. 18 S: Property distributions and circulation in the South Indian Ocean. *Deep-Sea Res.*, 28(8), 759-788, [https://doi.org/10.1016/S0198-0149\(81\)80001-5](https://doi.org/10.1016/S0198-0149(81)80001-5), 1981.

- Waser, N., Harrison, P., Nielsen, B., Calvert, S., and Turpin, D.: Nitrogen isotope fractionation during the uptake and assimilation of nitrate, nitrite, ammonium, and urea by a marine diatom. *Limnol. Oceanogr.*, 43(2), 215-224, <https://doi.org/10.4319/lo.1998.43.2.0215>, 1998.
- Williams, R. G., and Follows, M. J.: The Ekman transfer of nutrients and maintenance of new production over the North Atlantic. *Deep-Sea Res. Pt. I*, 45(2-3), 461-489, [https://doi.org/10.1016/S0967-0637\(97\)00094-0](https://doi.org/10.1016/S0967-0637(97)00094-0), 1998.
- Williams, R. G., and Follows, M. J.: Physical transport of nutrients and the maintenance of biological production *Ocean biogeochemistry* (pp. 19-51): Springer, 2003.
- Woodberry, K. E., Luther, M. E., and O'Brien, J. J.: The wind-driven seasonal circulation in the southern tropical Indian Ocean. *J. Geophys. Res.-Oceans*, 94(C12), 17985-18002, <https://doi.org/10.1029/JC094iC12p17985>, 1989.
- 10 Wurl, O.: Practical guidelines for the analysis of seawater: CRC press, 2009.
- Wüst, G.: Die Stratosphäre. Wissenschaftliche Ergebnisse der Deutschen Atlantischen Expedition auf dem Vermessungs- und Forschungsschiff "Meteor" 1925-1927. 6(1,2), Jg., S. 109-288, 1935.
- Wyrtki, K.: The oxygen minima in relation to ocean circulation. Paper presented at the Deep Sea Research and Oceanographic Abstracts, [https://doi.org/10.1016/0011-7471\(62\)90243-7](https://doi.org/10.1016/0011-7471(62)90243-7), 1962.
- 15 Wyrtki, K.: Oceanographic atlas of the international Indian Ocean expedition: National Science Foundation, 1971.
- Wyrtki, K.: Physical oceanography of the Indian Ocean The biology of the Indian Ocean (pp. 18-36): Springer. https://doi.org/10.1007/978-3-642-65468-8_3, 1973.
- You, Y.: Intermediate water circulation and ventilation of the Indian Ocean derived from water-mass contributions. *J. Mar. Res.*, 56(5), 1029-1067. <https://doi.org/10.1357/002224098765173455>, 1998.
- 20 You, Y., and Tomczak, M.: Thermocline circulation and ventilation in the Indian Ocean derived from water mass analysis. *Deep-Sea Res. Pt. I*, 40(1), 13-56. [https://doi.org/10.1016/0967-0637\(93\)90052-5](https://doi.org/10.1016/0967-0637(93)90052-5), 1993.

← **Formatiert:** Reference, Block, Einzug: Links: 0 cm, Hängend: 0,5 cm, Zeilenabstand: 1,5 Zeilen